Agricultural and Forest Meteorology 375 (2025) 110858

Contents lists available at ScienceDirect

Agricultural and Forest Meteorology

journal homepage: www.elsevier.com/locate/agrformet

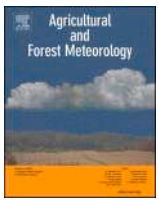

Mediterranean strictly protected forests are cooler

Francesco Solano [a], Chiara Mansi [b], Michele Baliva [b], Daniele Canestrelli [b], Alessandro Chiarucci [c], Raffaele Manicone [d], Maurizio Maugeri [e], Giuseppe Modica [f], Jordan Palli [b,*], Giovanni Quilghini [g], Gianluca Piovesan [b]

[a] Department of Agriculture and Forest Sciences, University of Tuscia, via San Camillo de Lellis s/n, 01100 Viterbo, Italy
[b] Department of Ecological and Biological Sciences, University of Tuscia, Largo dell'Università s/n, 01100 Viterbo, Italy
[c] BIOME Lab, Department of Biological, Geological, and Environmental Sciences, Alma Mater Studiorum - University of Bologna, Via Irnerio 42, Bologna 40126, Italy
[d] Comando Unità Forestali Ambientali ed Agroalimentari (CUFAA), Raggruppamento Carabinieri Biodiversità, Via Giosuè Carducci 5, 00187 Roma, Italy
[e] Department of Environmental Science and Policy, Università degli Studi di Milano, Via Celoria 10, 20133 Milan, Italy
[f] Dipartimento di Scienze Veterinarie, Università degli studi di Messina, Viale G. Palatucci s/n, I-98168 Messina, Italy
[g] Reparto Carabinieri Biodiversità Follonica, Via Bicocchi 2, 58022 Follonica, Italy

ARTICLE INFO

Keywords:
Climate mitigation
Forest resilience
Climate cooling
Remote sensing
Restoration outcomes
Effective management
Nature-based solutions
Rewilding

ABSTRACT

Forests are essential for climate mitigation and adaptation strategies. While the thermal buffering role of old-growth forests is well known, the long-term cooling benefits of restored forests in strictly protected areas remain poorly understood, particularly in the Mediterranean region – a biodiversity hotspot severely affected by climate change. In this paper, we examined summer maximum canopy temperatures using satellite observations across a Mediterranean forest landscape in Tuscany (Italy) during the period 2013–2023. Our analysis focused on topographic and forest attributes influencing temperature variations among evergreen oak stands under different IUCN management categories (Ia and V) compared to coppiced stands outside protected areas. The Ia site, legally established in 1961, is the first strictly protected reserve in the coastal Mediterranean. We observed measurable differences in canopy cooling at the mesoclimatic scale among strictly protected (IUCN Ia), protected landscape (IUCN V), and productive forests. Unmanaged stands with taller structure exhibited cooler conditions, with average summer maxima of 33.3 °C in strictly protected areas versus 35.4 °C in actively managed forests. Linear regression and GAM models suggest that terrain (elevation, aspect, topographic position index), forest structure (canopy height, tree cover), functional traits (canopy moisture content, EVI) and forest edge effects were the main factors affecting canopy maximum temperature. Even after accounting for topographical and stand attributes, productive forests were 1 °C warmer than strictly protected areas, underlying specific properties that emerge as these stands recover towards more natural stages. Our findings confirm canopy temperature as a robust proxy for assessing forests' biophysical role in moderating localized heat and evaluating restoration and conservation outcomes. This study underscores the urgent need to restore Mediterranean forests through strict protection, ensuring canopy-level thermal regulation and forest resilience. We advocate for area-based conservation and rewilding as essential nature-based solutions that integrate climate change mitigation and biodiversity protection within sustainable landscape management strategies.

1. Introduction

Global warming increases regional aridity and drought, threatening ecosystem functioning (IPCC, 2023). In this context, forests are key pillars for climate mitigation and adaptation (Gohr et al., 2021), as they regulate climate by adsorbing and stocking carbon (Mukul et al., 2020), enhancing the hydrological cycle, and cooling the temperature through increased evapotranspiration (Barnes et al., 2024). Moreover, forests create microclimates that can act as microrefugia for a wide range of organisms, buffering the impact of changing environments on individual species' performance (Nevins and Zambrano, 2024; Vandewiele et al., 2023). However, the sheltering and buffering potential of forests relies on maintaining ecosystem integrity, in which an intact and complex canopy structure plays a crucial role (John et al., 2024; De Lombaerde

* Corresponding author.
E-mail address: jo.palli@unitus.it (J. Palli).

https://doi.org/10.1016/j.agrformet.2025.110858
Received 15 July 2025; Received in revised form 29 August 2025; Accepted 18 September 2025
Available online 30 September 2025
0168-1923/© 2025 The Authors. Published by Elsevier B.V. This is an open access article under the CC BY license (http://creativecommons.org/licenses/by/4.0/).

et al., 2022). Disturbances to forest structure trigger thermophilization (Zellweger et al., 2020), destroying or altering the spatial and temporal variation of local microclimates (Máliš et al., 2023) and, consequently, microrefugia. Interactions between tree cover changes, habitat destruction, and other global change factors are exacerbating interconnected global crises of the Earth system (Mahecha et al., 2022). This is due to complex feedback loops between biodiversity decline and climate change, which are driving an increase in climate extremes (Barnes et al., 2024) and species loss (Betts et al., 2017).

Forest ecosystems play a crucial role in buffering climate extremes, thereby contributing to local and regional climate regulation (Lin et al., 2020; Sanczuk et al., 2023). Studies have shown that microclimatic conditions tend to be more variable in managed forest stands than in old-growth forests (Máliš et al., 2023). In primary and old-growth forests, the complex structure of vegetation creates a more stable environment, mitigating temperature fluctuations and maintaining moisture levels (Adhikari et al., 2025; Lindenmayer et al., 2022; Meli et al., 2024). This is particularly important in the context of climate change, as increased temperature extremes challenge ecosystem stability (Vacek et al., 2023). Notably, forests that have been under long-term protection demonstrate a greater cooling capacity than areas exposed to human disturbance or land use change (Adhikari et al., 2024; Xu et al., 2022). By reducing the impacts of climate extremes and sheltering particularly sensitive species from these impacts (McGinn et al., 2023), forests also play an essential role in safeguarding biodiversity (Corlett, 2020). The preservation of old-growth forests and the restoration of mature natural forests are therefore crucial not only for climate regulation, but also for preventing the loss of species that rely on stable, non-erratic environmental conditions.

The restoration of forest integrity has emerged as a promising nature-based solution to address both climate adaptation and biodiversity conservation (Lipka et al., 2023; Wright and Francia, 2024). As global environmental challenges intensify, restoring forests to a more natural state can enhance ecosystem resilience, mitigate climate extremes, and contribute to biodiversity recovery (Alibakhshi et al., 2024). In this context, rewilding stands in strictly protected areas - those where human exploitation is excluded - can provide valuable insights into how ecosystems can recover in the absence of direct human intervention. Despite growing recognition of the importance of strict protection and forest restoration for sustainable development (Hemraj et al., 2024), the time needed for full recovery of ecosystem functionality remains to be quantified. In fact, studies about the capacity of forests to cool the climate generally concern reforestation or old-growth forests (e.g., Barnes et al., 2024; Zhang et al., 2020), while the restoration dynamic toward natural ecosystems is still overlooked in many parts of the world. This lack of research particularly concerns regions in the Mediterranean basin, which is increasingly vulnerable to climate change (Cramer et al., 2018). The Mediterranean basin is a global biodiversity hotspot (IUCN, 2013) that is experiencing significantly faster summer warming than the global average, with an estimated amplification of around 40 %. This accelerated warming is linked to an increase in the frequency and intensity of summer heatwaves, more severe and prolonged droughts, and more intense heavy rainfall events (Urdiales-Flores et al., 2024). These stresses are exacerbated by centuries of land use changes and deforestation (Palli et al., 2023; Santi et al., 2024). Despite the region's importance and vulnerability, a notable gap remains in research focused on long-term forest restoration processes, particularly regarding the effectiveness of protected areas in mitigating climate impacts and restoring ecosystem resilience. In this context, the role of unmanaged rewilding forests in mitigating extreme warming events (Gohr et al., 2021) remains overlooked. Addressing this gap is crucial for developing tailored conservation strategies that help protect the region's unique biodiversity and contribute to broader climate adaptation goals in areas with high population density.

Satellite-derived land surface temperature (LST) offers a unique opportunity to evaluate the thermal behavior of forest canopies across large spatial and temporal scales. LST, derived from thermal infrared satellite data, provides a spatially explicit indicator of the temperature at the top of the canopy, reflecting how vegetation structure and function affect the energy balance at the land–atmosphere interface. Although LST does not directly represent air temperature or microclimatic conditions within the understory, it is a valuable proxy for assessing canopy-scale thermal regulation and the landscape-level impacts of forest cover on surface warming. Recent advances in Earth observation enable fine-scale assessment of how forest structure interacts with surface temperature dynamics (Basnet et al., 2025). This is particularly relevant for evaluating the outcomes of different forest management regimes, including strictly protected areas, extensive conservation zones, and actively managed forests such as coppices. Moreover, while the climatic benefits of forest conservation are well recognized at the global and regional levels (Peña-Claros and Nobre, 2023) their expression at the mesoclimatic scale – particularly in response to extreme heat events – remains poorly understood.

To fill this knowledge gap within Mediterranean ecosystems, we explored the climate mitigation capacity, as measured by the average summer maximum canopy temperature, of forest stands protected under different regimes, spanning from a strictly protected area (IUCN category Ia) to a protected landscape (IUCN category V) and non-protected productive coppices. Specifically, this paper addresses the following research questions:

- How do summer maximum forest canopy temperatures differ between strictly protected areas (IUCN Ia), protected landscapes (IUCN V), and non-protected forests managed for firewood production (coppicing) under Mediterranean climate?
- How do topographical characteristics (microsite) and canopy structural and functional attributes influence the cooling capacity of Mediterranean evergreen forests facing increasing aridity?
- Taking into account differences in microsite environment and remotely sensed forest attributes (e.g., height, canopy cover), does the level of protection provide greater capacity to mitigate the effects of heat waves? More specifically, what is the relationship between long-term rewilding (strict protection) and the mesoclimatic role of forest canopies in regulating surface temperature under severe summer heat stress conditions? Does the cooling effect of ecological restoration increase over time?

2. Materials and methods

2.1. Study area

The study area (Fig. 1) is the Poggio Tre Cancelli strict reserve (IUCN category Ia; hereafter SR), the second to be established in Italy in 1961 (Pavan, 1961; Administrative decree 07/26/1971) and the first one in the coastal zone of the Mediterranean basin (https://www.protectedplanet.net/5968, accessed on December 2024). SR extends for 99 ha along the Mediterranean coastal area in central-western Italy. The Reserve is managed by the Carabinieri Forestali Biodiversity Group. Located in the municipality of Follonica (Tuscany, Italy), SR is entirely included in the perimeter of the Interprovincial Park of Montioni (IUCN category V; hereafter NP) established in 1998 following the national framework park law 394/91. The area is characterized by a low hilly terrain, where calcareous marly reliefs range from 108 to 280 m a.s.l.

The area falls within the Mediterranean pluviseasonal oceanic bioclimatic variant, characterized by a lower mesomediterranean thermotype and a lower subhumid ombrotype (Pesaresi et al., 2017). It has a mean annual temperature of 15.4 °C and an average annual precipitation of 688 mm (Fig. 1). The current forest cover of the SR and NP is characterized by a stored coppice, derived from a long history of coppicing with standards management systems for firewood and charcoal supply. Indeed, the last logging activities date back to 1948 in a peripheral part of the SR (Pavan, 1961) while in the NP harvesting

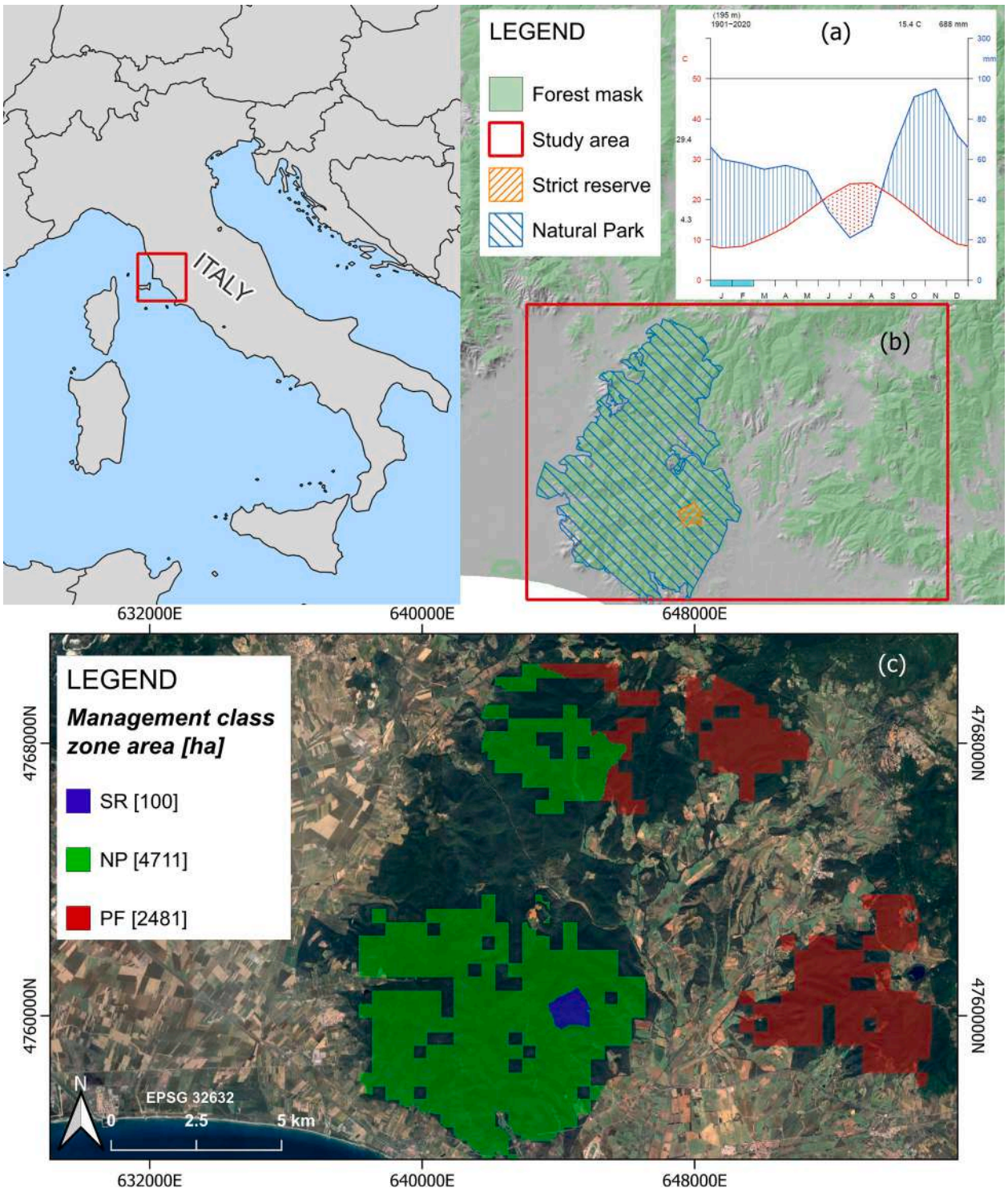

Fig. 1. Study area. (a) Walter and Lieth climate diagram showing temperature and precipitation curves from CRU data (http://badc.nerc.ac.uk/data/cru/) for the period 1901–2020. (b) Localization of the Poggio Tre Cancelli Strict Reserve (SR), the interprovincial Natural Park of Montioni (NP), and other forested areas outside the protected area. c); Forest mask layer areas considered in this study. Colored areas refer to management classes from the strict reserve (SR) and Natural Park (NP) to the productive forest (PF) of the same forest type (mixed sclerophyllous forest with *Quercus ilex* L. growing on calcareous marly reliefs).

activities stopped in the last decades. Coppicing with standards system is still practiced in the productive forest (hereafter PF) (Fig. 1). The dendrological tree species composition is characterized by the typical Mediterranean sclerophyllous vegetation dominated by holm oak (*Quercus ilex* L.) accompanied by strawberry tree (*Arbutus unedo* L.), south european flowering ash (*Fraxinus ornus* L.), black hornbeam (*Ostrya carpinifolia* Scop.) and turkey oaks (*Quercus cerris* L.). The NP and the PF have a similar tree species composition (see below).

2.2. Data acquisition and processing

To reach our goal, we designed a workflow (Fig.2) that can be summarized in the following main steps: (a) input data acquisition and processing; (b) harmonization of dependent and explanatory variables;

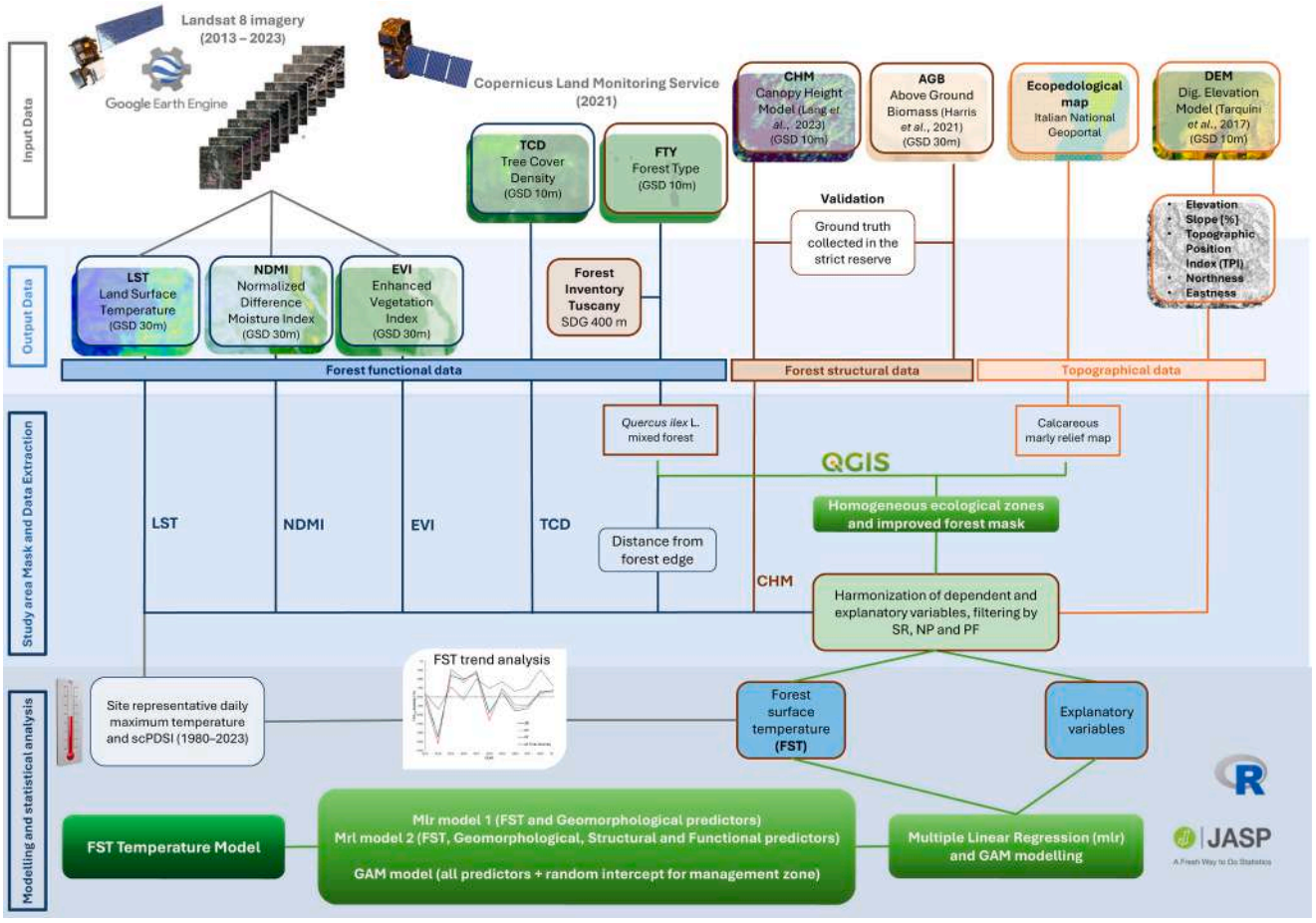

Fig. 2. Workflow of the study. Forest functional, structural, and topographical data and the forest surface temperature (FST) were derived from remotely sensed datasets.

(c) masking the study area forest land; (d) modeling land surface temperature (LST) via parametric statistical method.

2.2.1. *Study area forest mask for comparative analysis*

To investigate how forest protection status affects canopy thermal patterns, we defined a forest mask encompassing areas with comparable ecological conditions across a gradient of management intensity. We used official vector polygon boundaries of the SR provided by the Carabinieri Forestali Biodiversity Group, and of the NP (https://www502.regione.toscana.it/geoscopio/arprot.html, accessed on November 2023) to delineate the core protected areas (IUCN categories Ia and V, respectively). To extend the analysis beyond the protected core and include productive forests (PF), we focused on identifying forest stands that were ecologically and compositionally comparable to SR. To do so, we defined a search radius of 10 km around the SR. This distance was chosen because, within this range, it was still possible to find forest ecosystems with comparable composition, substrate, and mesoclimatic conditions, allowing meaningful comparisons without the confounding effects of biogeographical or climatic divergence (De Frenne et al., 2025). Within this area, we further used the vector polygons of the Italian ecopedological map from the National Geoportal (http://wms.pcn.minambiente.it/ogc?map=/ms_ogc/wfs/Carta_ecopedologica.map, accessed on: February 2024), to select only the areas belonging to the same ecopedological category of the strict reserve (calcareous marly reliefs). The Forest Type 2021 HRL forest layer (FTY) (https://land.copernicus.eu/en/products/high-resolution-layer-forests-and-tree-cover/forest-type-2021-raster-10-m-100-m-europe-3-yearly, accessed in November 2023) of the Copernicus Land Monitoring Service (CLMS) was used to further abstract reference forest areas. As the variability of the forest temperature is also influenced by the type of vegetation, we searched for vegetation similar to the SR (i.e., mixed sclerophyllous forest with *Quercus ilex* L.). To this aim, we used the regional Tuscany Forest Inventory with a spatial resolution of 400 m (https://dati.toscana.it/dataset/ucs/resource/92355190-d959–436c-92a6-e370950f915f, accessed in April 2024), selecting only forest cover dominated by holm oak. Based on on-screen photointerpretation of high-resolution Google Earth imagery and forest disturbance data product (Senf and Seidl, 2021a), we also masked forest area where disturbances (intended as forest-cutting activities) occurred during the period of investigation (https://doi.org/10.5281/zenodo.3924381. accessed on: May 2025). These filters ensured that selected productive forest sites (PF) outside the protected area were comparable to the SR, differing primarily in their management regime. The resulting forest mask (Fig. 2) thus enabled a robust comparative analysis of canopy thermal responses across gradients of protection and management intensity (Fig. 2).

2.2.2. *Land surface temperature (LST) estimation*

LST was retrieved from NASA's Landsat 8 OLI/TIRS satellite imagery by developing a JavaScript code in the Google Earth Engine (GEE) cloud computing environment (Gorelick et al., 2017). We used atmospherically corrected and orthorectified surface reflectance and thermal infrared bands of the USGS Landsat 8 Level 2, Collection 1, Tier 1 imagery (https://developers.google.com/earth-engine/datasets/catalog/LANDSAT_LC08_C02_T1_L2#description, accessed on November 2024) acquired in the summer period (1 June-31 August) from 2013 to 2023 for a total of 143 scenes. After applying the proper scaling and offset factor to all optical and thermal bands, we masked out cloud and cloud shadow-affected pixels by using the QA_PIXEL quality attributes band

generated from the CFMASK algorithm (Foga et al., 2017), and the collection was reduced by the maximum value of each pixel across the stack. To retrieve LST from the Landsat thermal band, we implemented a standard mono-window LST retrieval algorithm by established procedures (e.g., Sobrino et al., 2004; Jimenez-Munoz et al., 2009) which estimate and correct the land surface emissivity to account for its spatial variability resulting from different vegetation cover within each pixel. First, we derived the fraction of vegetation cover (Pv) from the NDVI (normalized difference vegetation index) calculated over the image collection using near infra-red (Band 5 - NIR) and red (Band 4 - RED) bands as follows:

$$NDVI = \frac{NIR - RED}{NIR + RED}$$

and the proportion of vegetation (Pv) was calculated as

$$Pv = \left(\frac{NDVI - NDVI_{min}}{NDVI_{max} - NDVI_{min}}\right)^2$$

where $NDVI_{max}$ is the maximum NDVI value and $NDVI_{min}$ is the minimum NDVI value. Then, the land surface emissivity (ε) was computed with the following equation:

$$\varepsilon = mP_v + n$$

In the emissivity equation, m is a proportionality coefficient that reflects the difference between vegetation and soil emissivity, adjusted by the geometrical shape factor (F), while n represents the baseline emissivity derived from a weighted combination of soil and vegetation values. Specifically, $m = (\varepsilon_v - \varepsilon_s) - (1 - \varepsilon_s)\, F\varepsilon_v$ and $n = \varepsilon_s + (1 - \varepsilon_s)\, F\varepsilon_v$, where ε_v is the vegetation emissivity, ε_s is the soil emissivity, F the shape factor, and P_v is the proportion of vegetation. Following Sobrino et al. (2004), we set $m = 0.004$, $n = 0.986$, and $F = 0.55$, assuming the mean of different geometrical distributions. NDVI was not directly used to correct or model LST, which was derived from thermal infrared radiance, making it primarily a function of surface temperature, not vegetation greenness per se. Finally, the maximum per-pixel LST at 30 m ground sample distance (GSD) over the study area was computed as follows:

$$LST = \frac{T_b}{\left[1 + \left(\lambda \frac{T_b}{\rho}\right)\right] \times ln\varepsilon} - 273.15$$

where T_b is the thermal band brightness temperature (in Kelvin), λ is the central band wavelength at which radiance is emitted ($\lambda = 10.8$ μm, by NASA); $\rho = h \times c/\sigma$ (1.438×10^{-2} m K) with h being Planck's constant (6.626×10^{-34} J·s), c is the velocity of light (2.998×10^{8} m·s^{-1}), σ is the Boltzmann constant (1.38×10^{-23} J·K^{-1}), and ε is the calculated emissivity. The value of 273.15 was subtracted from the resulting LST in Kelvin to convert it to Celsius degrees (°C). The improved study area mask was then used to obtain a forest surface temperature (hereafter FST) map representing LST data of the forest canopy within the study area.

2.2.3. Forest structural parameters

Spatially explicit forest canopy height (CHM) and above-ground woody biomass (AGB) maps were used to assess the forest structure (Table 1). In this paper, we used the CHM published by Lang et al. (2023). This dataset reports tree canopy heights at 10 m of GSD, developed by a probabilistic deep learning model coupling height data from the Global Ecosystem Dynamics Investigation (GEDI) space-borne LiDAR mission with Sentinel-2 optical satellite images. Despite the LST dataset covering a broader temporal range (2013–2023), we considered CHM to be representative of forest structure over the entire study period, given that the SR and NP areas are composed of mature, unmanaged stands where height change is minimal over decadal timescales. Forest AGB data were extracted from Harris et al. (2021), which reported biomass density (per hectare) at 30 m of GSD derived using a multi-step processing of LiDAR data with regional allometric equations and Landsat imagery. The CHM dataset was resampled by mean value to match the AGB dataset GSD (i.e., 30 m).

CHM and AGB data were validated through comparison with ground truth data provided by the Carabinieri Forestali Biodiversity Group of Follonica, collected along a 13,500 m^2 sample transect in the SR. Within the plot, all live and dead-standing trees were geolocated using a global navigation satellite system (GNSS) receiver. For each tree, the diameter at breast height (DBH, i.e. diameter above 1.30 m) and the total height were measured with a diameter caliper and an ultrasonic hypsometer, respectively. Tree volume (in m^3) and biomass (in Mg) were then calculated using species-specific allometric equations from the national forest inventory (NFI) (Tabacchi et al., 2011). This dataset was then imported into QGIS environment (QGIS Development Team, 2024) as a vector point, with the relative biomass and height attributes associated with each individual tree. A grid of 60 m x 60 m was superimposed over the transect, and single tree AGB values within the cell were aggregated (per hectare) for comparison with the raster's AGB value. To align our measurements with the canopy height model (CHM) raster data, we calculated the 98th percentile of the measured tree heights within each cell. This metric is consistent with the RH98 canopy-top height definition derived from GEDI L1B waveforms, as defined by Lang et al. (2023). Then, a linear regression analysis was performed to describe the relationships between remotely - derived data and field measurements over the transect.

2.2.4. Forest functional parameters and edge effect

Forest functional parameters were derived from the same NASA Landsat 8 OLI/TIRS satellite imagery collection described in Section 2.2.2. reduced by the median value across the stack. To quantify vegetation greenness, the Landsat 8 bands (B02, B04, B05, B06) were used to derive the enhanced vegetation index (EVI) (Table 1), which is strongly related to plant phenology and chlorophyll content (Huete et al., 2002). Also, the normalized difference moisture index (NDMI) (Table 1) was calculated to account for canopy water content (Gao, 1996). We used the Tree Cover Density 2021 HRL forest layer (TCD) (https://land.copernicus.eu/en/products/high-resolution-layer-forests-and-tree-cover/tree-cover-density-2021-raster-10-m-100-m-europe-yearly, accessed on November 2023) of the Copernicus Land Monitoring Service (CLMS) as the vertical projection of forest tree crowns to the horizontal Earth's surface. The TCD provides information on the proportional crown coverage per pixel at 10 m spatial resolution (100 m^2) in a continuous scale (0–100 %) and was resampled to a 30 m/pixel resolution by mean value. The TCD layer was considered in both structural and functional parameters (Solano et al., 2021). Finally, to consider the forest edge effect, which influences forest ecosystem functioning (Fischer et al., 2021; Wang et al., 2020), we calculated the distance between the forest boundary and the inner forest areas. The Forest Type 2021 HRL forest layer (FTY) (https://land.copernicus.eu/en/products/high-resolution-layer-forests-and-tree-cover/forest-type-2021-raster-10-m-100-m-europe-3-yearly, accessed on November 2023) of the Copernicus Land Monitoring Service (CLMS) was used as reference forest mask as it provide a map with "forest" pixel classified following the forest definition of the Food and Agriculture Organization (FAO, 2023) with a GSD of 10 m (100 m^2). The FTY was then resampled to 30 m spatial resolution (900 m^2) by mean value and the forest border was derived via QGIS software. Then, we calculated the distance from the forest boundary as the distance from the center of each forest pixel to the center of the nearest pixel identified as non-forest.

2.2.5. Geomorphological and topographical parameters

Bare ground surface morphology was included in the FST modeling to account for topography, elevation, slope and aspect influences on vegetation structures and dynamics (Cheng et al., 2023). From the TINITALY DEM (Tarquini and Nannipieri, 2017) raster data, with a 10 m

cell size (Version 1.1; https://doi.org/10.13127/tinitaly/1.1) we calculated the slope (in %) and the aspect. The aspect was then transformed into eastness and northness. Eastness was calculated as sin (aspect), indicating the east/west direction of the slope, while northness was calculated as cos(aspect), indicating the north/south direction of the slope (Wilson et al., 2007). The DEM was also used to calculate the topographic position index (TPI), which quantifies a location's relative position by comparing its elevation to the average elevation of the surrounding area within a specified radius. This method allows for identifying landscape features such as ridges, valleys, and flat areas. The TPI calculation was performed following the methodology outlined by Weiss (2001), where positive TPI values indicate locations higher than the surrounding terrain (e.g., ridges), negative values represent lower areas (e.g., valleys), and values near zero suggest flat or constant slope regions. All datasets were projected to the UTM zone 32 N, WGS 84 (EPSG 32,632) coordinate reference system. All candidate predictor variables layers were then co-registered using the basic pixel alignment algorithm of the image-to-image automatic co-registration processing QGIS plugin (https://github.com/SMByC/Coregistration-Qgis-processing, accessed in February 2024) and the final improved study area mask was then used to extract potential predictor variables data in the four forest management class zones. All geomorphological and topographical parameters are summarized in Table 1.

2.2.6. Climatological anomalies trend analysis and FST_{max} yearly variation

Site-representative free-air daily temperature series between 1980 and 2023 were obtained by employing the anomaly method, which assumes that the daily temperatures of any point can be expressed by summing two independent components: the climate normal over a given reference period (i.e., the 30-arc-second temperature climatology of Brunetti et al. (2014) and the deviations from it (i.e., the anomalies). Site representative anomalies of maximum free-air temperature during summer ($T_{max}A$) were obtained by calculating a weighted average of the anomalies from the stations in the Brunetti et al. (2006) dataset, incorporating the station networks of the Italian Air Force and various Italian regional agencies. Our rationale for using the anomaly approach was to investigate how and to what extent heatwave extremes, which are ecologically impactful and increasingly frequent under climate change maximum, impact forest surface temperature during summer (FST_{max}anomaly).

$T_{max}A$ and FST_{max}anomaly trends were analyzed by fitting a least-squares regression and assessed by using the non-parametric Mann-Kendall (MK) method, which has been widely used in climate studies (Kendall, 1975; Mann, 1945). The MK test statistic (*S*) was used to determine the sign (positive or negative) of an existing trend, and the *Z* statistic was used to determine whether a trend was significant or not (at the $\alpha = 0.05$ level). We analyzed the long-term trend of time series of $T_{max}A$ from the 1980–2023, which represent the departure from the long-term average reference value. Then, we conducted the trend analysis on the common period 2013–2023. To investigate the strength and direction of the relationship between the $T_{max}A$ and the satellite-derived FST_{max} among the different management zones, we used the Spearman's rank correlation coefficient (*rho* coefficient) calculated for the period 2013–2023, with a two-sided hypothesis test.

The relative climate dryness was assessed through the Palmer Drought Severity Index (PDSI) (Palmer, 1965). As PDSI is sensitive to different climate and land cover properties, we used its adapted formulation, the self-calibrated PDSI (scPDSI), which reduces the excessive frequency of extreme events by calibrating the original PDSI using local conditions (Wells et al., 2004). The monthly scPDSI dataset for the period 1901–2022 was downloaded from the CRU (https://crudata.uea.ac.uk/cru/data/drought/, accessed in April 2024) at a spatial resolution of 0.5 × 0.5 degrees (Dunn et al., 2022; van der Schrier et al., 2013). Trend analysis was conducted using the method described previously. The *rho* coefficient was also calculated between FST_{max} and the scPDSI to evaluate the impact of drought spells on maximum summer temperatures.

2.2.7. Statistical analysis and FST_{max} modeling

A non-parametric analysis of variance (ANOVA) was conducted using the Kruskal-Wallis test (Kruskal and Wallis, 1952) to assess significant differences in forest canopy temperatures across different levels of management intensity. Post-hoc comparisons were performed using

Table 1
List of candidate predictor variables used in this study for the Forest Surface Temperature (FST) modeling.

Candidate predictor	Description	Spatial resolution	Temporal resolution	References
Forest structural parameters				
Canopy Height Model - CHM	Canopy height data (in m) derived from RH98 NASA's Global Ecosystem Dynamics Investigation (GEDI) full waveform LiDAR and Sentinel-2 satellite imagery	10m	2020	Lang et al. 2023
Above ground biomass AGB	A global map of the aboveground biomass, density (megagrams biomass per ha) with a multi-step process composed by LiDAR data, regional allometric equations and based on Landsat imagery	30	2000	Harris et al., 2021
Forest functional parameters and edge effect				
Tree Cover Density (TCD)	Percentage of the canopy cover per pixel	10m	2021	Geospatial Data Catalogue Copernicus Land Monitoring Service (CLMS)
Enhanced Vegetation Index (EVI)	A vegetation greenness index $EVI = \frac{G * NIR - RED}{(NIR + C1 * RED - C2 * BLUE + L)}$	30m	2013 - 2023	Huete et al., 2002
Normalized Difference Moisture Index (NDMI)	Vegetation index related to water content $NDMI = \frac{(NIR - SWIR)}{(NIR + SWIR)}$	30m	2013 - 2023	Gao, 1996
Distance from forest edge	The minimum distance of a single pixel from the forest edge (in km)			Fischer et al., 2021; Wang et al., 2020
Geomorphological and topographical parameters				
Elevation	Elevation of the bare ground	10m	2023	Tarquini et al., 2017
Topographic Position Index (TPI)	Difference between the elevation of the center point and the average elevation of its surrounding neighbors	10m	2023	Weiss, 2001
Northness	The cosine of aspect	10m	2023	Wilson et al., 2007
Eastness	The sin of aspect	10m	2023	Wilson et al., 2007
Slope	Percentage of inclined surface	10m	2023	
Response				
Forest Surface Temperature (FST)	Measurement of the emission of thermal radiance from the land surface (in this case forest canopy surface).	30m	2013 - 2023	United States Geological Survey (USGS) NASA

the Dunn's z-test (Dunn, 1964), with *p*-values adjusted using the Benjamini-Hochberg correction (Benjaminit and Hochberg, 1995) for multiple testing. Moreover, we performed a test for the comparison of the coefficients of variation of FST_{max} among the management classes following Forkman (2009).

Prior to the FST_{max} modeling, we explored data distribution via univariate statistics, correlation analysis among FST_{max} and all candidate predictors, and checked for multiple regression assumptions to be satisfied. Multicollinearity between the independent variables was assessed using tolerance statistics and the Variance Inflation Factor (VIF), and variables with a VIF > 5 were discarded (O'brien, 2007). Linear regression was used to investigate the effects of covariates (site and forest attributes) and factors (forest management classes). We then ran two multiple regression models: The first was built by including only the elevation, slope, TPI, eastness, and northness predictor variables to test if, given the same environment, the protection regime may influence the FST_{max}. The second was built by adding all the other functional and structural predictor variables to model their effect on temperature. The study area management classes were used as a factor for both models.

To assess the potential non-linearity in the relationships between candidate predictors and FST_{max}, we implemented Generalized Additive Models (GAMs). GAMs allow for flexible, data-driven estimation of smooth relationships between predictors and response variables, without assuming a priori linearity (Wood, 2017). The response variable was FST_{max} (°C), and the predictors included the comprehensive set of topographic, structural, and functional forest attributes. Each of these variables was modeled as a smooth term using thin plate regression splines, allowing for smooth but spatially invariant effects across the study area. To account for unobserved heterogeneity between forest zones, a random intercept for zone was included, allowing to adjust for baseline differences in FST_{max} among zones. The general structure of the model was:

$$FST_{max} = \beta_0 + \sum s(X_i) + b_{management_{class}} + \varepsilon$$

where $s(Xi)$ represents the global smooth function of each continuous predictor, and $b_{management\_class}$ represents a random effect associated with each management zone. The degree of smoothing was selected via restricted maximum likelihood (REML), and model assumptions were assessed via residual diagnostics.

Statistical analyses were performed using JASP software (JASP Team, 2023) and the *mgcv, tidyverse* packages in R (R Core Team, 2024).

3. Results

3.1. Strict reserve forest structure and remote sensing data validation

The SR is dominated by holm oak, and it is characterized by an uneven-aged forest structure (Fig. S1). The average DBH is 16.5 cm (± 9.4) with a predominant height (sensu Ford et al., 2007) of 27 m (± 0.8). The tree basal area is 22 m^2 ha^{-1} and a total volume of 193 m^3 ha^{-1} was estimated, corresponding to 139 Mg ha^{-1} of woody biomass. Considering the time since the last cutting (75 years), the average increase in volume is equal to 2.573 m^3 ha^{-1} yr^{-1}, underlying the low productivity of this forest stand.

CHM validation showed a statistically significant strong relationship with the 98th percentile of measured tree height ($R^2 = 0.86$, $F(1,13) = 77.72$, $p < 0.001$), supporting its use in the following analysis (Fig. S2). The correlation between measured AGB and the global AGB dataset was not significant ($R^2 = 0.024$, $F(1,13) = 0.32$, $p = 0.581$) and suggested that global data may underestimate the measured woody biomass (Fig. S2). For this reason, the AGB data was not used in the modeling phase.

3.2. FST_{max} variation and free air temperature trend analysis

During the study period (2013–2023), FST_{max} varied from an average value of 33.3 °C (± 0.5) in the SR, 34.2 °C (± 1.1) in the NP to 35.4 °C (± 2.3) in the PF (Fig. 3). The highest FST_{max} (49.2 °C) was registered within the PF, decreasing to 34.3 °C in the SR. More in general, the FST_{max} are higher in PF compared to protected areas (Fig. 3 and Fig. S3). The strict reserve (SR) consistently records the lowest FST_{max} during hot summers (Fig. 3 and Fig. S3). The Kruskal-Wallis test revealed significant differences in FST_{max} among the forest management classes (Fig. 3). Thus, we rejected the null hypothesis and assumed there were differences between the different protection regimes in terms of summer daily maximum surface temperatures during the considered period, as confirmed by Dunn's post-hoc test (Fig.3). SR is also distinguished by the lowest year-to-year variation in FST_{max} (Fig 3; Fig. S4). The zones within the Natural Park exhibit canopy temperature dynamics that are intermediate between the SR and productive coppice forests (PF).

The $T_{max}A$ series exhibited a significant upward trend from 1980 to 2023, accounting for 43.9 % of the variance in temperature anomalies (Fig. S5). When considering only the data that coincide with FST_{max} measurements derived from satellites, the trend line for 2013–2023 indicates an upward trend. However, the trend is not significant due to large year-to-year variability (Fig. S5). Overall, trend analysis highlighted the increasing temperature extremes over the past four decades, with a tendency towards more pronounced extremes in recent years.

The correlation analysis (Fig. S6) shows strong, significant correlations between FST_{max} across various forest management classes, especially within NP and SR. This suggests a consistent response to regional climate variations. However, there's no significant correlation between $T_{max}A$ and FST_{max}. Despite this, all forest management types tend to show positive temperature anomalies during hot and severe drought periods (indicated by negative scPDSI values in Fig. S7), though the correlation with scPDSI is also not significant (Fig. S7).

The most influential predictors of FST_{max} are directly related to the amount, density, and health of the vegetation (TCD, EVI, CHM, NDMI), all of which demonstrate strong negative correlations with FST (Fig. 4). Proximity to forest edges also significantly influences FST_{max}, with interior forest areas generally being cooler. Topographical factors (Elevation, Slope, Northness, Eastness, TPI) show weaker correlations, suggesting they are less dominant drivers of FST compared to vegetation characteristics.

3.3. Disentangling factors for temperature differences among forest management classes

Descriptive statistics of the topographical (Elevation, Slope, Eastness, Northness, TPI), forest structural (CHM), functional (TCD, EVI, NDMI), and distance from the forest edge (Edge distance) parameters highlighted significant differences between management classes (Fig. S8).

The linear model developed to explain variation in FST_{max} using topographic variables and categorical zoning (Tab. S1), accounts for 35.1 % of the total variance in FST (Adjusted $R^2 = 0.351$) and is statistically significant ($F(7, 81{,}813) = 6334.255$, $p < 0.001$). The Root Mean Square Error (RMSE) of the model is 1.420. Elevation, slope, and northness showed significant negative associations with FST_{max}, while eastness and TPI were positively associated. Multicollinearity was not critical, as demonstrated by the Tolerance (86 % - 99 %) and VIF values (<1.2). Forest management classes were significant factors influencing the FST_{max}, which increased from SR to PF (2.0 °C) (Tab. S1). When adding to the model the structural, functional and forest edge effect predictors, the model accounted for 79.6 % of the variance in FST_{max} (Adjusted $R^2 = 0.796$; RMSE = 0.796; $p < 0.001$; Table 2). Elevation, slope, northness, CHM, TCD, NDMI, and edge distance were significantly negatively associated with FST_{max}, whereas eastness, TPI, and EVI had

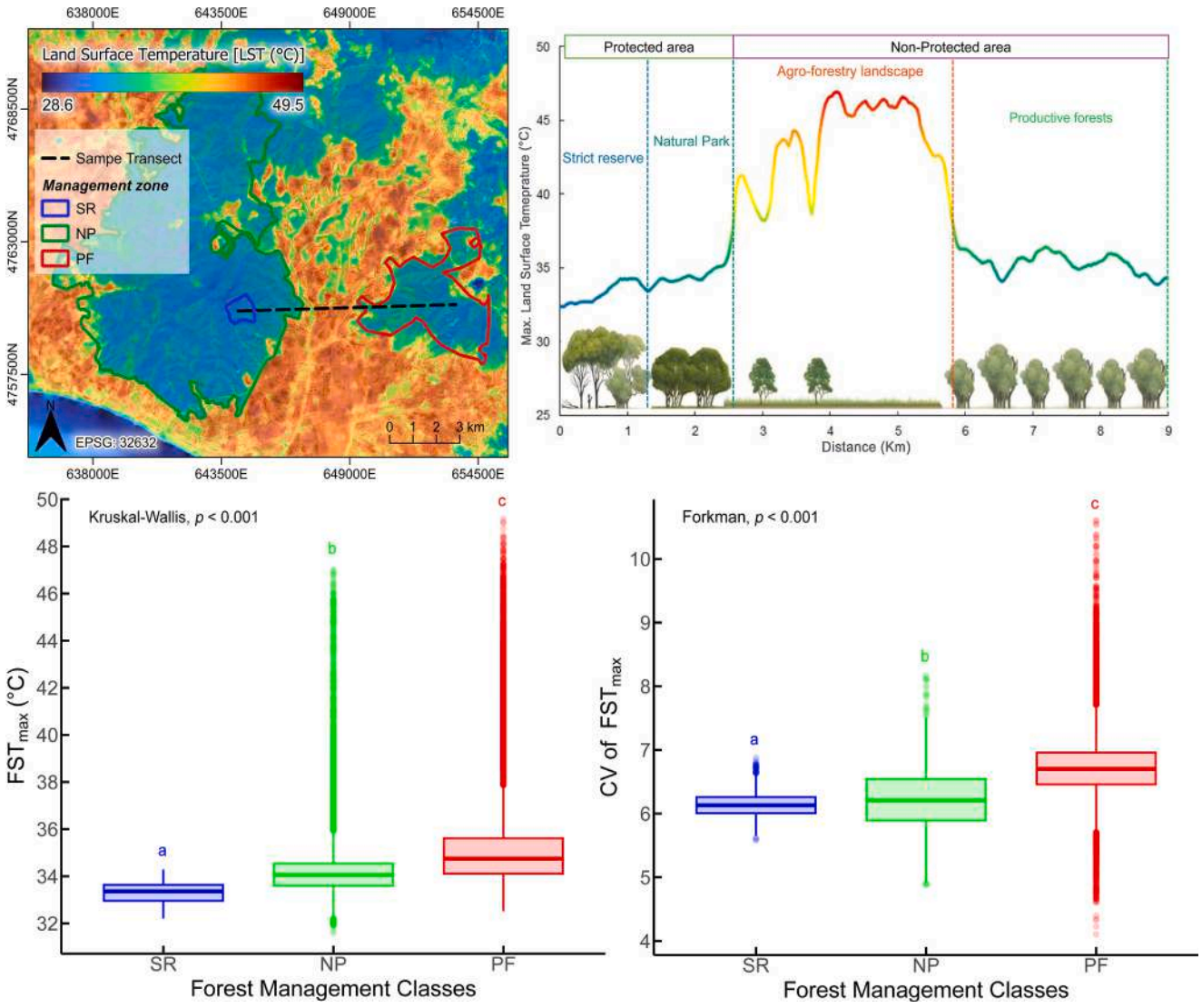

Fig. 3. Spatial and statistical analysis of maximum forest surface temperature (FST_{max}) across three forest management zones: strict reserve (SR), natural park (NP), and productive forest (PF). Top-left: Land Surface Temperature (LST) map derived from remote sensing data, with colored boundaries indicating the three management zones (SR, NP, PF). Top-right: LST values along a representative transect, showing the thermal gradient from the SR to adjacent agro-forestry and managed forest areas (PF) and highlighting localized thermal patterns and spatial variability. Bottom-left: boxplot of FST_{max} across zones. Bottom-right: boxplot of the coefficient of variation (CV) of FST_{max}, representing intra-zone thermal heterogeneity. Different letters above boxplots indicate statistically significant differences among groups (Kruskal–Wallis test with Dunn's post-hoc comparisons, $p < 0.001$, for FST_{max}, Forkman test for CV of FST_{max}).

positive effects. The temperature offset was modeled as an increase up to 1.14 °C on average in the case of PF compared to SR. There was no collinearity among predictors, with tolerance values ranging from 0.42 to 0.95 and the largest VIF value of 2.3.

The GAM with a Tweedie distribution ($p = 1.99$) and a logarithmic link function explained 85.7 % of the deviance in FST_{max}, with an adjusted R^2 of 0.858 indicating robust predictive power. All predictor variables included as smooth terms were highly significant ($p < 0.001$) revealing complex non-linear relationships with FST_{max} (Table 3a and Fig. 5). Among the predictors, NDMI, distance to forest edge, eastness, elevation, and CHM showed the strongest effects on FST. The random effect for management zone was associated with a very large F-value ($F = 7238.03$), confirming a leading role of forest management class in determining surface temperature patterns, independent of other environmental predictors (Table 3b). The PF zone showed the highest average FST (effect = +0.0163). The NP exhibited a slightly lower FST (effect = −0.0058) and the SR recorded the lowest FST (effect = −0.0106). Predicted FST_{max} was 33.52 °C in SR, 33.73 °C in NP (+0.21 °C vs. SR), and 34.53 °C in PF (+1.01 °C), with narrow 95 % confidence intervals in all cases (Table 3b).

Model diagnostics (Fig. S9 and S10) prove the improvement in residual assumptions, validating the sufficiency of basis dimensions for all smooth terms.

CHM and NDMI both showed strong negative relationships with FST, indicating that taller canopies and higher moisture content are associated with lower surface temperatures. Distance from forest edge had a strong negative effect on FST, with cooler temperatures found in forest interiors revealing a localized marked influence up to 250–500 m from the edge (Fig. 5). Elevation and slope showed clear negative effects on FST, with higher altitudes and steeper slopes associated with cooler surface temperatures (Fig. 5). TPI displayed a positive trend at higher values, suggesting warmer conditions on convex terrain. Northness and eastness exhibited non-linear relationships suggesting that south and east facing slopes experience warmer FST. FST increased rapidly with tree canopy density (TCD) and EVI up to a plateau.

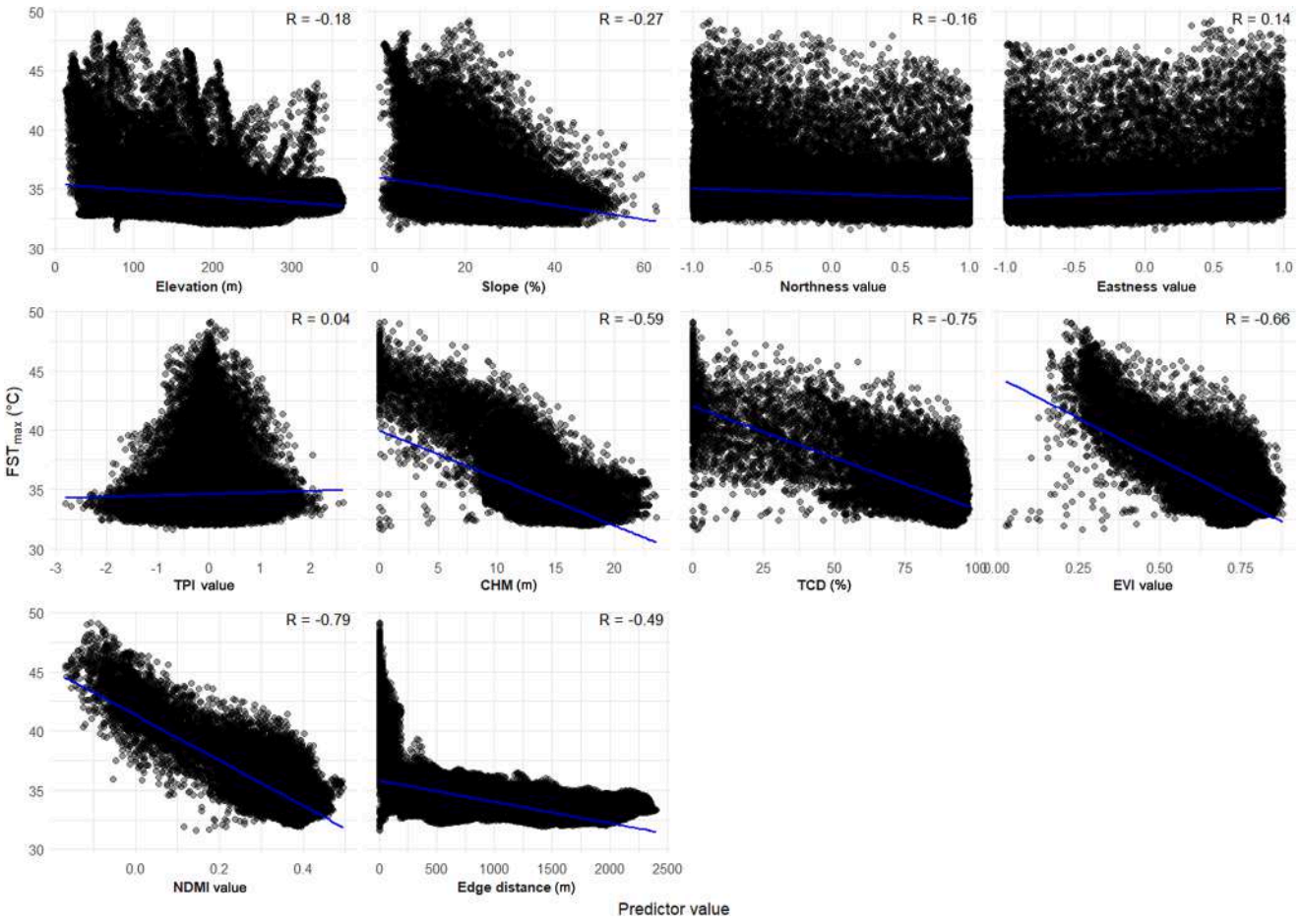

Fig. 4. Scatter plots of the relationships between forest surface temperature (FST_{max}) and topographical, structural, functional, and forest edge effect, along with their respective Pearson correlation coefficients (*R* values). All reported correlations are statistically significant ($p < 0.001$).

Table 2
Summary table of multiple regression model predicting FST_{max} based on the value of topographical, structural, functional, and edge effect predictors. Management classes were considered factor variables. SR is the reference site.

							Collinearity Statistics	
Model		Unstandardized	Standard Error	Standardized	t	p	Tolerance	VIF
H_0	(Intercept)	34.613	0.006		5617.2	<0.001		
H_1	(Intercept)	41.617	0.04		1043.6	<0.001		
	Elevation	−0.002	6.129×10^{-5}	−0.071	−32.5	<0.001	0.719	1.391
	Slope	−0.011	3.671×10^{-4}	−0.048	−28.7	<0.001	0.955	1.048
	Northness	−0.035	0.005	−0.013	−7.3	<0.001	0.911	1.098
	Eastness	0.364	0.005	0.135	77.8	<0.001	0.913	1.096
	TPI	0.073	0.005	0.025	15	<0.001	0.937	1.067
	CHM	−0.086	0.002	−0.128	−57.5	<0.001	0.712	1.405
	TCD	−0.018	4.215×10^{-4}	−0.156	−43.1	<0.001	0.436	2.292
	EVI	0.994	0.072	0.047	13.8	<0.001	0.469	2.133
	NDMI	−13.012	0.09	−0.536	−144.2	<0.001	0.425	2.352
	Edge distance	−57.14	7.607×10^{-6}	−0.143	−69.8	<0.001	0.769	1.3
	Forest management classes							
	NP	0.13	0.025		5.1	<0.001		
	PF	1.145	0.026		44.6	<0.001		

4. Discussions

4.1. Differences in canopy maximum temperature between forest management classes

Our analysis revealed significant variations in forest canopy maximum surface temperatures (FST_{max}) across a Mediterranean coastal landscape in central Italy during the summer months. These variations were observed among forest stands with differing levels of protection and management practices. In particular, the SR (IUCN 1a) stand provides compelling evidence of the significant cooling/buffering capacity effect of a forest stand managed as a strictly protected area and undergoing a long-term rewilding process compared to harvested and human disturbed stands. In addition, the SR stand showed a distinctive thermal

Table 3
a) Generalized Additive Model (GAM) results for FST_{max} prediction. ***$p < 0.001$. b) Predicted FSTmax for different management zones. FST predictions were calculated by holding all other continuous predictors at their mean value in the dataset. Strict Reserve (SR) is used as the reference zone for calculating differences.

a)

Predictor term	Effect type	edf (Effective Degrees of Freedom)	F-statistic
(Intercept)	Parametric	N/A	N/A
s(Elevation)	Smooth	8.84	700.21***
s(Slope)	Smooth	4.5	216.71***
s(Northness)	Smooth	8.15	133.55***
s(Easteness)	Smooth	8.07	819.22***
s(TPI)	Smooth	6.45	128.07***
s(CHM)	Smooth	8.9	605.76***
s(TCD)	Smooth	2	85.41***
s(EVI)	Smooth	8.89	195.21***
s(NDMI)	Smooth	8.91	2031.94***
s(Edge distance)	Smooth	17.84	1511.42***
s(Forest management classes)	Random effect	1.99	7238.03***

b)

Forest management class	Predicted FST (°C)	95 % Confidence lower interval (°C)	95 % Confidence upper interval (°C)	Difference from Reference Zone (SR) (°C)
SR	33.52	33.46795	33.57765	N/A
NP	33.73	33.68928	33.76589	0.21
PF	34.53	34.48746	34.56717	1.01

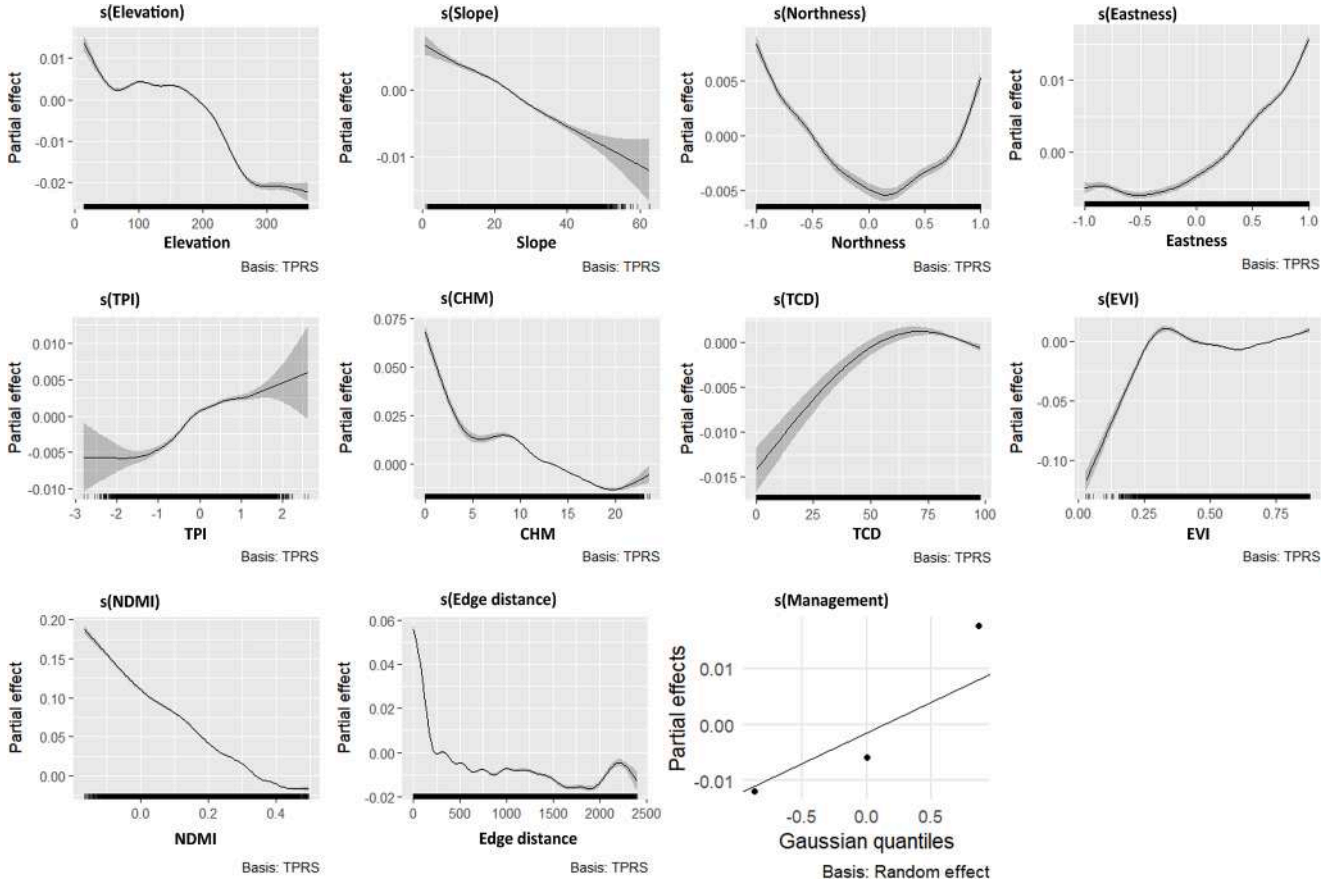

Fig. 5. Partial effects of predictors on maximum forest surface temperature (FST_{max}) as estimated by the GAM. Each panel displays the estimated smooth function (black line) for a given predictor on the log-linked scale, along with its 95 % confidence interval (grey shaded area). The tick marks along the x-axis represent the density of observations (rug plot). The final panel, s(Management), shows the estimated random effects for different management zones against Gaussian quantiles.

stability, crucial for preserving biodiversity and ecological processes (Lindenmayer et al., 2022; Wolf et al., 2021), which are often disrupted by temperature fluctuations in managed forests (Máliš et al., 2023). This compelling evidence underscores the critical role of protected areas in mitigating the effects of global climate change (Huang et al., 2022; Lehikoinen et al., 2021; Xu et al., 2022) and highlights the substantial benefits of long-term, strict protection in enhancing restoration outcomes (Hemraj et al., 2024) by facilitating the recovery of functional ecosystems.

In this area, with vegetation characterized by evergreen forest adapted to summer drought and a relatively high species richness, especially for woody species (Chiarucci and Bonini, 2005), climate is the main driver of species composition and is likely to be significantly affected by climate change (Arévalo et al., 2012). After more than sixty

years of strict protection, the SR forest ecosystem has restored a tall canopy and, as a result, the summer daily maximum temperature is 2 °C lower compared to adjacent stands being actively managed for wood production. Even when considering all the analyzed environmental, structural and functional conditions, the SR remains cooler by approximately 1 °C. Natural Park areas (NP, i.e., IUCN V) also consistently recorded lower FST_{max}, compared to productive forest areas, in agreement with previous studies (Adhikari et al., 2024; Blumröder et al., 2021; Haight and Hammill, 2020; Santi et al., 2024). These results highlight the role of conservative management in maintaining a stronger canopy cooling effect and the importance of preserving and restoring complex forest structures, which are also essential for ecosystem resilience (Baliva et al., 2024). The implications of these findings are relevant for mitigating the increasing frequency of extreme heat and drought in the Mediterranean basin (Suarez-Gutierrez et al., 2023). Indeed, the trend analysis of maximum air temperatures on a multi-decadal scale revealed a remarkable increase in T_{max} anomalies, in agreement with global warming (Hansen et al., 2023).

Areas managed with intensive forestry practices (coppice with standards) showed higher surface temperatures, as shorter tree canopies, and fragmentation/edge effects reduce the cooling effect compared to a more natural complex forest ecosystem (Greiser et al., 2020; Javadian et al., 2022). The result of this study aligns with broader observations that disturbed forests tend to be about 1.5 °C warmer than their undisturbed counterparts (Santos et al., 2024). Taller complex canopies, such as those found in the SR, contribute to lower surface temperatures through high surface roughness that enhances turbulent exchange, leading to increased evapotranspiration (Mildrexler et al., 2011). In contrast, warmer temperatures characterizing intensively harvested areas such as productive coppice forests are explained by the shorter structure and open canopy patch, which also increases their vulnerability to global changes (Thom et al., 2020). This study confirmed that forest cover and stand structure modulate the impact of external maximum temperatures, providing a natural cooling effect that varies depending on management practices and biomes (i.e., becoming more relevant towards the tropics; De Lombaerde et al., 2022).

It is worth noting that temperature variations between different protection and management classes persist even when the descriptive parameters of the environmental, structural, and functional characteristics of the stand are included in the models. While this discrepancy may stem from limitations in the remote-sensing derived covariates, recent studies have highlighted the emergence of novel ecological qualities in forest ecosystems that exhibit a higher degree of naturalness. For instance, mature and old-growth forests exhibit greater drought resistance and a better ability to sustain water availability compared to younger stands, which are more sensitive to climate variations (Adhikari et al., 2024; Farinacci et al., 2024). As vegetation dynamics of unmanaged stands progresses toward more natural conditions, a range of microhabitats and microclimates emerge within the forest ecosystem (Kovács et al., 2024), enhancing the overall forest resilience to climate change, particularly in Mediterranean environments (Baliva et al., 2024; Colangelo et al., 2021). Also noteworthy is the putative facilitating role of large and old trees, which have survived in the perturbed forests, acting as true hubs for the ecosystem's resilient responses (Piovesan et al., 2022).

The small average FST_{max} difference between SR and NP suggests that most of the thermal buffer capacity can be recovered in a few decades (30–40 years), as shown in case studies of the recovering forest landscape in the eastern United States (Zhang et al., 2020). However, in the Mediterranean environment, about 75 years after coppicing has ceased, the unmanaged stored coppice continues to cool, probably because low biomass growth rates that slow down the structural restoration processes of complex, tall forests rich in large and old trees. Considering that an old-growth holm oak forest in Sardinia exhibits more than twice the above-ground biomass (340 t ha^{-1}) (François and Terradas, 2013) compared to that measured at Tre Cancelli Strict Reserve and given the holm oak's remarkable longevity (Filibeck et al., 2023), the return to a high level of naturalness will still require a significant amount of time. However, the absence of an old-growth reference forest within the study area severely limits our ability to predict a substantial increase in future surface cooling capacity. This study underscores discrepancies between local (based on site tree measurements) and global biomass estimates, with the latter underestimating carbon sequestration, particularly in primary forests (Ralhan et al., 2023). More accurate biomass estimates are crucial for efficient forest management, supporting conservation priorities and enhancing carbon sequestration strategies.

4.2. Drivers of summer maximum temperature buffering

The correlation between $T_{max}A$ and FST_{max} was positive but not significant, confirming that along with air temperature, relevant environmental factors and forest attributes influence the temperature of the forest canopy (e.g. water balance; Davis et al., 2019).

A first key result of this study is that severe disturbances to the forest canopy – such as those produced by intensive coppicing activities – alter the natural forest mesoclimate and microclimate by increasing the solar radiation reaching the ground (Vandewiele et al., 2023) and reducing the distance of core forest areas from the edges (Máliš et al., 2023). Therefore, the contrasting CHM characteristics across management zones provide a key biophysical explanation for the observed inter-zonal differences in FST, underscoring how management practices that influence forest vertical structure ultimately modulate the thermal environment. Restoring coppiced forests towards a more complex canopy structure may be adopted as a "win-win" nature-based solution, as it combines conservation and adaptation goals, providing a resilient context that can effectively address the challenges of climate change mitigation and biodiversity protection (Lipka et al., 2023).

Beyond the direct influence of forest structure, our models highlighted the significant role of NDMI in modulating FST_{max}. A strong negative relationship was observed, where low NDMI values (indicating drier canopy conditions) were associated with a significant positive effect on FST, resulting in warmer surface temperatures. Conversely, as NDMI increased (reflecting higher moisture content in vegetation and soil), the effect on FST rapidly leads to cooler surfaces. This finding robustly underscores the critical importance of moisture availability in the forest thermal regime (Senf and Seidl, 2021b; Vandewiele et al., 2023). Areas with higher water content dissipate more energy through evapotranspiration, thereby effectively cooling the surface. This mechanism is particularly vital in Mediterranean environments, where water availability is a primary limiting factor and directly influences vegetation's ability to buffer thermal extremes (Mu et al., 2021; Sungmin et al., 2022). This suggests that taller canopies and higher moisture content are essential for maintaining lower maximum temperatures (Zhang et al., 2022) and the overall forest functionality and health, especially in the Mediterranean area. Indeed, the microclimate of forests is influenced by water supply (Manzi et al., 2024) and in particular, by (i) leaf evapotranspiration that contributes to mitigating extreme temperature events (De Frenne, 2023), and (ii) the cooling effect of tree trunks, which derives from the sap flux within the tree (Frey et al., 2023). The cooling effect of forests is related to ecosystem ecohydrology, where trees extract, recycle, and store water, thereby maintaining an optimal temperature range (Ellison et al., 2024). However, the sensitivity to regulate canopy temperature may differ across species, with a wide variability in hydraulic traits (Yi et al., 2020).

Small distances from the forest edge were associated with a strong positive effect on FST_{max}, indicating notably warmer temperatures right at the forest–non-forest boundary. This warming effect rapidly diminished as distance from the edge increased, eventually leveling off or showing minor fluctuations further into the forest interior. This strong "edge effect" is likely due to a combination of factors. Forest edges typically experience increased exposure to direct solar radiation,

reduced shading from adjacent canopy, higher air temperatures due to reduced buffering capacity, and altered wind patterns compared to the interior (Franklin et al., 2021; Meeussen et al., 2021). This increased energy input and reduced capacity for heat dissipation collectively contribute to the observed elevation in FST at the forest margins. The rapid decline of this warming effect with increasing distance highlights the localized nature of edge-induced microclimatic changes and the buffering capacity of the forest interior. Proximity to forest edges (e.g., adjacent agricultural fields, forest roads, firebreaks, or other infrastructures) negatively impacts microclimate stability with a strong non-linear effect extending up to 250 m. Thus, the edge effect becomes very relevant in fragmented forest landscapes (Dantas De Paula et al., 2016; Hending et al., 2023). Mitigating the impact of global warming and other factors contributing to forest degradation (e.g., alien species, human-made fires) requires large, undisturbed forest core areas. Forest disturbances that reduce canopy cover can dramatically alter the forest mesoclimate, and restoring the original structure and its temperature-buffering capacity may take decades (Vandewiele et al., 2023) – or even centuries in the case of fragmented forests in Mediterranean environments.

However, in semi-natural, closed-canopy forest landscapes, the Poggio Tre Cancelli strict reserve demonstrates that just a few decades can be sufficient to recover substantial climate-buffering capacity (see also Máliš et al., 2023). This kind of recovery dynamic, however, is largely feasible only within strictly protected areas, which currently represent a relatively small portion of EU territory and are mostly concentrated in high-altitude regions (Cazzolla Gatti et al., 2023). Consequently, expanding the coverage of strictly protected areas up to 10 % of the EU land area by 2030, with a focus on supporting rewilding processes, can not only enhance ecosystem resilience and maintain biodiversity (Perino et al., 2019) but also contribute significantly to climate change mitigation.

An intriguing finding from the GAM was the non-linear and positive response of FST_{max} to TCD and EVI. While an overall cooling effect of increased vegetation is widely recognized in many ecosystems (De Lombaerde et al., 2022), which contributes to regulating surface temperatures (Vandewiele et al., 2023) and the conservation of specialized forest understory communities (Lorer et al., 2024; Santi et al., 2024), our model revealed a more complex pattern for TCD and EVI.

The Generalized Additive Model (GAM) analysis revealed a positive, non-linear relationship between FST and canopy closure, a metric captured by both Tree Canopy Density (TCD) and the Enhanced Vegetation Index (EVI) (Fig. 5). This complex relationship, which emerged after checking other variables, suggests that the underlying biophysical processes are far more intricate than simple shading. For example, dense evergreen canopies, such as those of *Quercus ilex*, naturally have a low leaf albedo (darker leaves), leading to greater solar energy absorption as tree cover increases (Godinho et al., 2016). The albedo effect is compounded during periods of heat and drought by a significant reduction in evapotranspiration, which diminishes the forest's primary cooling mechanism. This highlights key ecophysiological limits in warm, drought-limited environments like the Mediterranean or the tropics, where extreme heat may trigger stomatal closure (Manzi et al., 2024). During heatwaves, this combination of high solar absorption and reduced evapotranspiration may explain why the cooling effect of canopy cover decreases up to a plateau at higher canopy densities. This effect negates the benefits of high greenness, as recently demonstrated in urban vegetation (Weng et al., 2025). However, this interpretative hypothesis requires further verification and in-depth study.

As expected, elevation significantly influences the climate, as it tends to lower mean temperatures and diminish the severity of temperature extremes. Previous studies indicated that higher-elevation areas tend to maintain cooler temperatures compared to lower-altitude areas, due to the adiabatic cooling process and decreased exposure to extreme events (Dobrowski, 2011). This combined process is particularly relevant in Mediterranean forests, where reliefs host refugial habitats for heat-sensitive species (Alston et al., 2020; Lovari et al., 2020; Malagnino et al., 2024), sheltering them during periods of intense warming.

The aspect influences the amount of solar radiation received, which in turn affects soil and canopy temperatures. North-facing aspects tend to stay cooler compared to south-facing ones, where solar radiation is more direct. This effect is well-documented in the literature: slopes with lower sun exposure tend to maintain cooler temperatures, making them especially suitable as microrefugia for species that depend on shaded, cooler conditions (Máliš et al., 2023). In this sense, forests with northern exposure or sheltered zones can be crucial for biodiversity conservation, as they offer natural climatic refuges for forest species. In this study, the marked canopy level cooling effect of the west aspect can be linked to the proximity to the Tyrrhenian Sea, generating cooling breeze and occult rain (Bernardino et al., 2022). Valleys and enclosed areas with negative TPI values tend to be cooler and more humid, favoring the creation of micro-refuges capable of maintaining stable thermal conditions. Studies have shown that areas with negative TPI values show lower temperatures than exposed ridges (Weiss, 2001). This suggests that TPI might help identify areas particularly favorable for maintaining stable mesoclimate conditions, that are essential for the ecological resilience of forest habitats and the protection of sensitive species. Together, these topographical parameters contribute to climatic diversity within forests, creating a range of environments that can act as micro-refuges for different species. This environmental heterogeneity is particularly important in the context of climate change, where natural forests can serve as "buffer zones" against extreme temperatures. Studies such as De Frenne et al. (2021) emphasize the importance of conserving habitats with these topographical characteristics as part of adaptation strategies, as they support natural resilience against global warming. Within complex terrain, old-growth forests and recovering forest ecosystems can synergistically provide crucial refuges for species to persist amidst a warming climate (Greiser et al., 2024). Considering the unprecedented rapid change in climatic conditions (IPCC, 2023), forest-assisted migration is seen as one of the solutions to help species migrate faster (Williams and Dumroese, 2013) and adapt to the new range margins. Our temperature-based assessment underscores the significant potential of forest restoration practices for local climate mitigation, a crucial aspect often overlooked in current forest-related pledges and policies aimed at addressing global warming. Forest managers and decision-makers play a pivotal role, as their choices significantly influence biodiversity conservation and the functioning of ecosystems (Menge et al., 2023), both of which are deeply impacted by the climate within the forest canopy (De Frenne et al., 2021).

Our results demonstrate that canopy temperature measured through remote sensing can serve as a key functional indicator for monitoring ecosystem recovery and the associated increase in ecosystem services, thus aiding in assessing the success of nature-based solutions in achieving environmental policy objectives (Hua et al., 2022; Sutherland et al., 2016). These findings suggest that strict protection and passive rewilding can significantly enhance forests' ecological functions by buffering the climate warming rate (Xu et al., 2022), in agreement with other recent findings that revealed the greater resilience of strictly protected areas to disturbances (Li et al., 2024).

5. Concluding remarks

This study unequivocally demonstrates the paramount importance of unmanaged forest sites in the face of accelerating global change, to provide fundamental ecosystem functions such as climate mitigation. Strictly protected areas demonstrated a greater thermal buffering capacity and reduced vulnerability to temperature extremes. Our findings reveal a significant cooling effect at the canopy scale of a Mediterranean strictly protected area, with summer maximum temperatures observed to be approximately 2 °C lower in a naturally recovering forest compared to a managed coppice forest. Various environmental and biophysical factors influence the modulation of forest surface

temperature, providing critical insights for forest management and climate change adaptation strategies. Key predictors, including topographical, structural, functional and forest edge effect variables exhibited highly significant non-linear effects on FST. Drier conditions and shorter canopies consistently led to higher FST, emphasizing the critical role of water availability and tall forest structure in maintaining cooler thermal regimes. The significant "edge effect" also highlighted a localized warming at forest boundaries, likely due to increased exposure and reduced buffering capacity.

Mediterranean forests play a vital role in local climate regulation, and their capacity to modulate FST is intricately tied to their structural complexity and moisture status. The mesoclimatic thermal benefits observed in strictly protected areas underscore the importance of conservation-oriented forest management in preserving critical thermal refugia in Mediterranean environment. These insights are invaluable for informing sustainable forest management strategies aimed at enhancing ecosystem resilience and mitigating the impacts of rising temperatures in a changing climate. Future research should consider incorporating detailed temporal analyses to fully capture seasonal and inter-annual FST dynamics and investigate the link between microclimate stability and biodiversity to inform conservation strategies.

CRediT authorship contribution statement

Francesco Solano: Writing – review & editing, Writing – original draft, Visualization, Validation, Software, Methodology, Investigation, Formal analysis, Data curation, Conceptualization. **Chiara Mansi:** Writing – review & editing, Writing – original draft, Software, Formal analysis, Data curation. **Michele Baliva:** Writing – review & editing, Software, Formal analysis. **Daniele Canestrelli:** Writing – review & editing, Writing – original draft, Validation, Investigation. **Alessandro Chiarucci:** Writing – review & editing, Writing – original draft, Validation, Investigation. **Raffaele Manicone:** Writing – review & editing, Resources. **Maurizio Maugeri:** Writing – review & editing, Writing – original draft, Validation, Resources, Investigation. **Giuseppe Modica:** Writing – review & editing, Writing – original draft, Validation, Investigation. **Jordan Palli:** Writing – review & editing, Writing – original draft, Visualization. **Giovanni Quilghini:** Writing – review & editing, Resources. **Gianluca Piovesan:** Writing – review & editing, Writing – original draft, Validation, Supervision, Methodology, Investigation, Funding acquisition, Formal analysis, Conceptualization.

Declaration of competing interest

The authors declare that they have no known competing financial interests or personal relationships that could have appeared to influence the work reported in this paper.

Acknowledgements

Francesco Solano were supported by the European Union - NextGenerationEU through the Italian Ministry of University and Research under PNRR) – Missione 4 Componente 2, Project code: CN00000022) within the Agritech National Research Center. Chiara Mansi was supported by the Department of Ecological and Biological Sciences of the University of Tuscia (D.M.373). GP and AC were partially supported by the European Union - NextGenerationEU through the Italian Ministry of University and Research under PNRR - M4C2-I1.4 Project code: CN00000033, Title: NBFC - National Biodiversity Future Center (CUP: J83C22000860007 and CUP: J33C22001190001) and by BANDO PRIN 2022 _ Shifting Paradigms: Biodiversity Law, Ecological Primacy and the Redefinition of Sustainability in the European Green Deal (CUP: J53D23006310006). All the authors warmly thank Dr. Bruno Bellisario (Univeristy of Tuscia) for his support in developing the GAM and in the interpretation of model outcomes. We also thank the anonymous reviewers for their constructive comments, which substantially improved the quality of the manuscript.

Supplementary materials

Supplementary material associated with this article can be found, in the online version, at doi:10.1016/j.agrformet.2025.110858.

Data availability

Data will be made available on request.

References

Adhikari, Y., Bachstein, N., Gohr, C., Blumröder, J.S., Meier, C., Ibisch, P.L., 2024. Old-growth beech forests in Germany as cool islands in a warming landscape. Sci. Rep 14 (1), 30311. https://doi.org/10.1038/s41598-024-81209-0.

Adhikari, Y., Blumröder, J.S., Meier, C., Ibisch, P.L., 2025. Beech buffers: microclimate regulation in temperate old-growth forests, surroundings and forest edge. Ecol. Indic 178, 114111. https://doi.org/10.1016/J.ECOLIND.2025.114111.

Alibakhshi, S., Cook-Patton, S.C., Davin, E., Maeda, E.E., Araújo, M.B., Heinlein, D., Heiskanen, J., Pellikka, P., Crowther, T.W., 2024. Natural forest regeneration is projected to reduce local temperatures. Commun. Earth. Environ. 5 (1). https://doi.org/10.1038/s43247-024-01737-5.

Alston, J.M., Joyce, M.J., Merkle, J.A., Moen, R.A., 2020. Temperature shapes movement and habitat selection by a heat-sensitive ungulate. Landsc. Ecol 35 (9), 1961–1973. https://doi.org/10.1007/s10980-020-01072-y.

Arévalo, J.R., Cortés-Selva, F., Chiarucci, A., 2012. Ecological determinants of species composition in the forest vegetation of Tuscany, Italy. Plant. Ecol. Evol 145 (3), 323–331. https://doi.org/10.5091/plecevo.2012.688.

Baliva, M., Palli, J., Perri, F., Iovino, F., Luzzi, G., Piovesan, G., 2024. The return of tall forests: reconstructing the canopy resilience of an extensively harvested primary forest in Mediterranean mountains. Sci. Total. Environ. 953, 175806. https://doi.org/10.1016/j.scitotenv.2024.175806.

Barnes, M.L., Zhang, Q., Robeson, S.M., Young, L., Burakowski, E.A., Oishi, A.C., Stoy, P. C., Katul, G., Novick, K.A., 2024. A century of reforestation reduced anthropogenic warming in the eastern United States. Earth's. Future 12 (2). https://doi.org/10.1029/2023EF003663.

Basnet, P., Grieger, S., Putzenlechner, B., Seidel, D., 2025. Forests with high structural complexity contribute more to land surface cooling: empirical support for management for complexity. J. For. Res. 36 (1), 1–16. https://doi.org/10.1007/S11676-025-01855-6/FIGURES/1.

Benjaminit, Y., Hochberg, Y., 1995. Controlling the false discovery rate: a practical and powerful approach to multiple testing. J. R. Stat. Soc. B:. Stat. Methodol. 57 (1), 289–300. https://doi.org/10.1111/J.2517-6161.1995.TB02031.X.

Bernardino, A.Di, Iannarelli, A.M., Casadio, S., Pisacane, G., Mevi, G., Cacciani, M., 2022. Classification of synoptic and local-scale wind patterns using k-means clustering in a Tyrrhenian coastal area (Italy). Meteorol. Atmos. Phys. 134 (2), 30. https://doi.org/10.1007/s00703-022-00871-z.

Betts, M.G., Wolf, C., Ripple, W.J., Phalan, B., Millers, K.A., Duarte, A., Butchart, S.H.M., Levi, T., 2017. Global forest loss disproportionately erodes biodiversity in intact landscapes. Nature 547 (7664), 441–444. https://doi.org/10.1038/nature23285.

Blumröder, J.S., May, F., Härdtle, W., Ibisch, P.L., 2021. Forestry contributed to warming of forest ecosystems in northern Germany during the extreme summers of 2018 and 2019. Ecol. Solut. Evid. 2 (3). https://doi.org/10.1002/2688-8319.12087.

Brunetti, M., Maugeri, M., Monti, F., Nanni, T., 2006. Temperature and precipitation variability in Italy in the last two centuries from homogenised instrumental time series. Int. J. Climatol. 26 (3), 345–381. https://doi.org/10.1002/joc.1251.

Brunetti, M., Maugeri, M., Nanni, T., Simolo, C., Spinoni, J., 2014. High-resolution temperature climatology for Italy: interpolation method intercomparison. Int. J. Climatol. 34 (4), 1278–1296. https://doi.org/10.1002/joc.3764.

Cazzolla Gatti, R., Zannini, P., Piovesan, G., Alessi, N., Basset, A., Beierkuhnlein, C., Di Musciano, M., Field, R., Halley, J.M., Hoffmann, S., Iaria, J., Kallimanis, A., Lövei, G. L., Morera, A., Provenzale, A., Rocchini, D., Vetaas, O.R., Chiarucci, A., 2023. Analysing the distribution of strictly protected areas toward the EU2030 target. Biodivers. Conserv 32 (10), 3157–3174. https://doi.org/10.1007/S10531-023-02644-5/FIGURES/6.

Cheng, Z., Aakala, T., Larjavaara, M., 2023. Elevation, aspect, and slope influence woody vegetation structure and composition but not species richness in a human-influenced landscape in northwestern Yunnan, China. Front. For. Glob. Change 6. https://doi.org/10.3389/ffgc.2023.1187724.

Chiarucci, A., Bonini, I., 2005. Quantitative floristics as a tool for the assessment of plant diversity in Tuscan forests. For. Ecol. Manage 212 (1–3), 160–170. https://doi.org/10.1016/j.foreco.2005.03.041.

Colangelo, M., Camarero, J.J., Gazol, A., Piovesan, G., Borghetti, M., Baliva, M., Gentilesca, T., Rita, A., Schettino, A., Ripullone, F., 2021. Mediterranean old-growth forests exhibit resistance to climate warming. Sci. Total. Environ. 801, 149684. https://doi.org/10.1016/J.SCITOTENV.2021.149684.

Corlett, R.T., 2020. Safeguarding our future by protecting biodiversity. Plant. Divers. 42 (4), 221–228. https://doi.org/10.1016/j.pld.2020.04.002.

Cramer, W., Guiot, J., Fader, M., Garrabou, J., Gattuso, J.-P., Iglesias, A., Lange, M.A., Lionello, P., Llasat, M.C., Paz, S., Peñuelas, J., Snoussi, M., Toreti, A., Tsimplis, M.N., Xoplaki, E., 2018. Climate change and interconnected risks to sustainable

development in the Mediterranean. Nat. Clim. Chang 8 (11), 972–980. https://doi.org/10.1038/s41558-018-0299-2.
Dantas De Paula, M., Groeneveld, J., Huth, A., 2016. The extent of edge effects in fragmented landscapes: insights from satellite measurements of tree cover. Ecol. Indic 69, 196–204. https://doi.org/10.1016/J.ECOLIND.2016.04.018.
Davis, K.T., Dobrowski, S.Z., Holden, Z.A., Higuera, P.E., Abatzoglou, J.T., 2019. Microclimatic buffering in forests of the future: the role of local water balance. Ecography 42 (1), 1–11. https://doi.org/10.1111/ecog.03836.
De Frenne, P., 2023. Novel light regimes in European forests. Nat. Ecol. Evol. 8 (2), 196–202. https://doi.org/10.1038/s41559-023-02242-2.
De Frenne, P., Beugnon, R., Klinges, D., Lenoir, J., Niittynen, P., Pincebourde, S., Senior, R.A., Aalto, J., Chytrý, K., Gillingham, P.K., Greiser, C., Gril, E., Haesen, S., Kearney, M., Kopecký, M., le Roux, P.C., Luoto, M., Maclean, I., Man, M., Van Meerbeek, K., 2025. Ten practical guidelines for microclimate research in terrestrial ecosystems. Methods. Ecol. Evol. 16 (2), 269–294. https://doi.org/10.1111/2041-210X.14476;WGROUP:STRING:PUBLICATION.
De Frenne, P., Lenoir, J., Luoto, M., Scheffers, B.R., Zellweger, F., Aalto, J., Ashcroft, M. B., Christiansen, D.M., Decocq, G., Pauw, K.De, Govaert, S., Greiser, C., Gril, E., Hampe, A., Jucker, T., Klinges, D.H., Koelemeijer, I.A., Lembrechts, J.J., Marrec, R., Hylander, K., 2021. Forest microclimates and climate change: importance, drivers and future research agenda. In: Global Change Biology, 27. Blackwell Publishing Ltd, pp. 2279–2297. https://doi.org/10.1111/gcb.15569.
De Lombaerde, E., Vangansbeke, P., Lenoir, J., Meerbeek, K.Van, Lembrechts, J., Rodríguez-Sánchez, F., Luoto, M., Scheffers, B., Haesen, S., Aalto, J., Christiansen, D. M., Pauw, K.De, Depauw, L., Govaert, S., Greiser, C., Hampe, A., Hylander, K., Klinges, D., Koelemeijer, I., Frenne, De, P., 2022. Maintaining forest cover to enhance temperature buffering under future climate change. Sci. Total. Environ. 810, 151338. https://doi.org/10.1016/j.scitotenv.2021.151338.
Dobrowski, S., 2011. A climatic basis for microrefugia: the influence of terrain on climate. Glob. Chang. Biol 17 (2), 1022–1035. https://doi.org/10.1111/j.1365-2486.2010.02263.x.
Dunn, O.J., 1964. Multiple comparisons using rank sums. Technometrics 6 (3), 241–252. https://doi.org/10.1080/00401706.1964.10490181.
Dunn, R.J.H., Aldred, F., Gobron, N., Miller, J.B., Willett, K.M., Ades, M., Adler, R., Allan, R.P., Anderson, J., Anneville, O., Aono, Y., Argüez, A., Arosio, C., Augustine, J.A., Azorin-Molina, C., Barichivich, J., Basu, A., Beck, H.E., Bellouin, N., Zotta, R.M., 2022. Global Climate. Bull. Am. Meteorol. Soc. 103 (8), S11–S142. https://doi.org/10.1175/BAMS-D-22-0092.1.
Ellison, D., Pokorný, J., Wild, M., 2024. Even cooler insights: on the power of forests to (water the Earth and) cool the planet. In: Global Change Biology, 30. John Wiley and Sons Inc. https://doi.org/10.1111/gcb.17195.
FAO, 2023. Terms and definitions FRA 2025. www.fao.org/forestry.
Farinacci, M.D., Jones, J., Silva, L.C.R., 2024. Carbon-water tradeoffs in old-growth and young forests of the Pacific Northwest. AGU. Adv. 5 (4). https://doi.org/10.1029/2024AV001188.
Filibeck, G., Baliva, M., Calcagnile, L., Chiarucci, A., D'Elia, M., Quarta, G., Quilghini, G., Piovesan, G., 2023. Rediscovering Montecristo's treasure: the island's holm oaks reveal exceptional longevity. Ecology 104 (7), e4064. https://doi.org/10.1002/ECY.4064.
Fischer, R., Taubert, F., Müller, M.S., Groeneveld, J., Lehmann, S., Wiegand, T., Huth, A., 2021. Accelerated forest fragmentation leads to critical increase in tropical forest edge area. Sci. Adv 7. https://www.science.org.
Foga, S., Scaramuzza, P.L., Guo, S., Zhu, Z., Dilley, R.D., Beckmann, T., Schmidt, G.L., Dwyer, J.L., Hughes, M.J., Laue, B., 2017. Cloud detection algorithm comparison and validation for operational Landsat data products. Remote. Sens. Env. 194, 379–390. https://doi.org/10.1016/j.rse.2017.03.026.
Ford, A.J., Brack, C., James, R.N., 2007. Site index prediction for *Pinus radiata* D.Don at local scale on the southern tablelands of New South Wales using a national forest productivity model. Aust. For. 70 (3), 152–157. https://doi.org/10.1080/00049158.2007.10675015.
Forkman, J., 2009. Estimator and tests for common coefficients of variation in normal distributions. Commun. Stat. -. Theory. Methods 38 (2), 233–251. https://doi.org/10.1080/03610920802187448.
François, R., Terradas, J., 2013. Quercus Ilex L. ecosystems: function, Dynamics and Management, 13. Springer Science & Business Media.
Franklin, C.M.A., Harper, K.A., Clarke, M.J., 2021. Trends in studies of edge influence on vegetation at humancreated and natural forest edges across time and space. Can. J. For. Res. 51 (2), 274–282. https://doi.org/10.1139/CJFR-2020-0308/SUPPL_FILE/CJFR-2020-0308SUPPLA.XLSX.
Frey, J., Holter, P., Kinzinger, L., Schindler, Z., Morhart, C., Kolbe, S., Werner, C., Seifert, T., 2023. Detailed mapping of below canopy surface temperatures in forests reveals new perspectives on microclimatic processes. Agric. Meteorol 341, 109656. https://doi.org/10.1016/j.agrformet.2023.109656.
Gao, B., 1996. NDWI—A normalized difference water index for remote sensing of vegetation liquid water from space. Remote. Sens. Env. 58 (3), 257–266. https://doi.org/10.1016/S0034-4257(96)00067-3.
Godinho, S., Gil, A., Guiomar, N., Costa, M.J., Neves, N., 2016. Assessing the role of Mediterranean evergreen oaks canopy cover in land surface albedo and temperature using a remote sensing-based approach. Appl. Geogr. 74, 84–94. https://doi.org/10.1016/J.APGEOG.2016.07.004.
Gohr, C., Blumröder, J.S., Sheil, D., Ibisch, P.L., 2021. Quantifying the mitigation of temperature extremes by forests and wetlands in a temperate landscape. Ecol. Inf. 66. https://doi.org/10.1016/j.ecoinf.2021.101442.
Gorelick, N., Hancher, M., Dixon, M., Ilyushchenko, S., Thau, D., Moore, R., 2017. Google Earth Engine: planetary-scale geospatial analysis for everyone. Remote. Sens. Env. 202, 18–27. https://doi.org/10.1016/j.rse.2017.06.031.
Greiser, C., Ehrlén, J., Meineri, E., Hylander, K., 2020. Hiding from the climate: characterizing microrefugia for boreal forest understory species. Glob. Chang. Biol. 26 (2), 471–483. https://doi.org/10.1111/gcb.14874.
Greiser, C., Hederová, L., Vico, G., Wild, J., Macek, M., Kopecký, M., 2024. Higher soil moisture increases microclimate temperature buffering in temperate broadleaf forests. Agric. Meteorol 345. https://doi.org/10.1016/j.agrformet.2023.109828.
Haight, J., Hammill, E., 2020. Protected areas as potential refugia for biodiversity under climatic change. Biol. Conserv 241, 108258. https://doi.org/10.1016/j.biocon.2019.108258.
Hansen, J.E., Sato, M., Simons, L., Nazarenko, L.S., Sangha, I., Kharecha, P., Zachos, J.C., von Schuckmann, K., Loeb, N.G., Osman, M.B., Jin, Q., Tselioudis, G., Jeong, E., Lacis, A., Ruedy, R., Russell, G., Cao, J., Li, J., 2023. Global warming in the pipeline. Oxf. Open. Clim. Change 3 (1). https://doi.org/10.1093/oxfclm/kgad008.
Harris, N.L., Gibbs, D.A., Baccini, A., Birdsey, R.A., de Bruin, S., Farina, M., Fatoyinbo, L., Hansen, M.C., Herold, M., Houghton, R.A., Potapov, P.V., Suarez, D.R., Roman-Cuesta, R.M., Saatchi, S.S., Slay, C.M., Turubanova, S.A., Tyukavina, A., 2021. Global maps of twenty-first century forest carbon fluxes. Nat. Clim. Chang 11 (3), 234–240. https://doi.org/10.1038/s41558-020-00976-6.
Hemraj, D.A., Bishop, M., Carstensen, J., Krause-Jensen, D., Stæhr, P.A.U., Russell, B.D., 2024. Nature protection must precede restoration. Science 383 (6679), 158. https://doi.org/10.1126/science.adn0543.
Hending, D., Randrianarison, H., Andriamavosoloarisoa, N.N.M., Ranohatra-Hending, C., Holderied, M., McCabe, G., Cotton, S., 2023. Forest fragmentation and its associated edge-effects reduce tree species diversity, size, and structural diversity in Madagascar's transitional forests. Biodivers. Conserv 32 (10), 3329–3353. https://doi.org/10.1007/S10531-023-02657-0. *2023 32:10*.
Hua, F., Adrian Bruijnzeel, L., Meli, P., Martin, P.A., Zhang, J., Nakagawa, S., Miao, X., Wang, W., McEvoy, C., Peña-Arancibia, J.L., Brancalion, P.H.S., Smith, P., Edwards, D.P., Balmford, A., 2022. The biodiversity and ecosystem service contributions and trade-offs of forest restoration approaches. Science 376 (6595), 839–844. https://doi.org/10.1126/SCIENCE.ABL4649.
Huang, A., Xu, X., Jia, G., Shen, R., 2022. Asymmetrical cooling effects of Amazonian protected areas across spatiotemporal scales. Environ. Res. Lett. 17 (5), 054038. https://doi.org/10.1088/1748-9326/AC6A6D.
Huete, A., Didan, K., Miura, T., Rodriguez, E.P., Gao, X., Ferreira, L.G., 2002. Overview of the radiometric and biophysical performance of the MODIS vegetation indices. Remote. Sens. Env. 83 (1–2), 195–213. https://doi.org/10.1016/S0034-4257(02)00096-2.
IPCC, 2023. Technical summary. Climate Change 2022 – Impacts, Adaptation and Vulnerability. Cambridge University Press, pp. 37–118. https://doi.org/10.1017/9781009325844.002.
IUCN, 2013. Red list Italian vertebrates. www.iucn.it.
JASP Team. (2023). *JASP* (0.18.1).
Javadian, M., Smith, W.K., Lee, K., Knowles, J.F., Scott, R.L., Fisher, J.B., Moore, D.J.P., van Leeuwen, W.J.D., Barron-Gafford, G., Behrangi, A., 2022. Canopy temperature is regulated by ecosystem structural traits and captures the ecohydrologic dynamics of a semiarid mixed conifer forest site. J. Geophys. Res.:. Biogeosciences 127 (2). https://doi.org/10.1029/2021JG006617.
Jimenez-Munoz, J.C., Cristobal, J., Sobrino, J.A., Soria, G., Ninyerola, M., Pons, X., 2009. Revision of the Single-Channel Algorithm for Land Surface Temperature Retrieval From Landsat Thermal-Infrared Data," in. IEEE Trans. Geosci. Remote Sens. 47 (1), 339–349. https://doi.org/10.1109/TGRS.2008.2007125.
John, A., Pradhan, K., Case, M.J., Ettinger, A.K., Hille Ris Lambers, J., 2024. Forest canopy cover affects microclimate buffering during an extreme heat event. Environ. Res. Commun. 6 (9), 091015. https://doi.org/10.1088/2515-7620/AD7705.
Kendall, M.G., 1975. Rank Correlation Methods, 4th edn. Charles Griffin, San Francisco, CA.
Kovács, B., Németh, C., Aszalós, R., Veres, K., 2024. Small oases below the canopy: the cooling effects of water-filled tree holes on the local microclimate in oak-dominated stands. Agric. Meteorol 353, 110058. https://doi.org/10.1016/j.agrformet.2024.110058.
Kruskal, W.H., Wallis, W.A., 1952. Use of ranks in one-criterion variance analysis. J. Am. Stat. Assoc 47 (260), 583. https://doi.org/10.2307/2280779.
Lang, N., Jetz, W., Schindler, K., Wegner, J.D., 2023. A high-resolution canopy height model of the Earth. Nat. Ecol. Evol. 7 (11), 1778–1789. https://doi.org/10.1038/s41559-023-02206-6.
Lehikoinen, P., Tiusanen, M., Santangeli, A., Rajasärkkä, A., Jaatinen, K., Valkama, J., Virkkala, R., Lehikoinen, A., 2021. Increasing protected area coverage mitigates climate-driven community changes. Biol. Conserv 253, 108892. https://doi.org/10.1016/J.BIOCON.2020.108892.
Li, G., Fang, C., Watson, J.E.M., Sun, S., Qi, W., Wang, Z., Liu, J., 2024. Mixed effectiveness of global protected areas in resisting habitat loss. Nat. Commun 15 (1), 1–17. https://doi.org/10.1038/s41467-024-52693-9. *2024 15:1*.
Lin, H., Tu, C., Fang, J., Gioli, B., Loubet, B., Gruening, C., Zhou, G., Beringer, J., Huang, J., Dušek, J., Liddell, M., Buysse, P., Shi, P., Song, Q., Han, S., Magliulo, V., Li, Y., Grace, J., 2020. Forests buffer thermal fluctuation better than non-forests. Agric. Meteorol 288–289. https://doi.org/10.1016/j.agrformet.2020.107994.
Lindenmayer, D., Blanchard, W., McBurney, L., Bowd, E., Youngentob, K., Marsh, K., Taylor, C., 2022. Stand age related differences in forest microclimate. For. Ecol. Manage 510, 120101. https://doi.org/10.1016/J.FORECO.2022.120101.
Lipka, O.N., Andreeva, A.P., Shishkina, T.B., 2023. Protected areas as nature-based solutions for climate change adaptation. ECAS 2023, 34. https://doi.org/10.3390/ecas2023-15659.
Lorer, E., Landuyt, D., Blondeel, H., Frenne, P.De, Verheyen, K., 2024. Forest floor environment overrules global change treatment effects on understorey communities

in a mesocosm experiment. Glob. Chang. Biol 30 (7). https://doi.org/10.1111/gcb.17443.
Lovari, S., Franceschi, S., Chiatante, G., Fattorini, L., Fattorini, N., Ferretti, F., 2020. Climatic changes and the fate of mountain herbivores. Clim. Change 162 (4), 2319–2337. https://doi.org/10.1007/s10584-020-02801-7.
Mahecha, M.D., Bastos, A., Bohn, F.J., Eisenhauer, N., Feilhauer, H., Hartmann, H., Hickler, T., Kalesse-Los, H., Migliavacca, M., Otto, F.E.L., Peng, J., Quaas, J., Tegen, I., Weigelt, A., Wendisch, M., Wirth, C., 2022. Biodiversity loss and climate extremes — study the feedbacks. Nature 612 (7938), 30–32. https://doi.org/10.1038/d41586-022-04152-y.
Malagnino, A., Courbin, N., Bonnot, N., Garel, M., Marchand, P., Morellet, N., Börger, L., Loison, A., 2024. The availability of thermal refuges shapes the thermoregulatory behavioural. tactic of a heat-sensitive alpine endotherm species. https://doi.org/10.21203/rs.3.rs-3923795/v1.
Máliš, F., Ujházy, K., Hederová, L., Ujházyová, M., Csölleová, L., Coomes, D.A., Zellweger, F., 2023. Microclimate variation and recovery time in managed and old-growth temperate forests. Agric. Meteorol 342, 109722. https://doi.org/10.1016/J.AGRFORMET.2023.109722.
Mann, H.B., 1945. Non parametric test against trend. Econometrica 13.
Manzi, O.J.L., Wittemann, M., Dusenge, M.E., Habimana, J., Manishimwe, A., Mujawamariya, M., Ntirugulirwa, B., Zibera, E., Tarvainen, L., Nsabimana, D., Wallin, G., Uddling, J., 2024. Canopy temperatures strongly overestimate leaf thermal safety margins of tropical trees. New. Phytol. 243 (6), 2115–2129. https://doi.org/10.1111/nph.20013.
McGinn, K.A., Peery, M.Z., Zulla, C.J., Berigan, W.J., Wilkinson, Z.A., Barry, J.M., Keane, J.J., Zuckerberg, B., 2023. A climate-vulnerable species uses cooler forest microclimates during heat waves. Biol. Conserv 283. https://doi.org/10.1016/j.biocon.2023.110132.
Meeussen, C., Govaert, S., Vanneste, T., Bollmann, K., Brunet, J., Calders, K., Cousins, S. A.O., De Pauw, K., Diekmann, M., Gasperini, C., Hedwall, P.O., Hylander, K., Iacopetti, G., Lenoir, J., Lindmo, S., Orczewska, A., Ponette, Q., Plue, J., Sanczuk, P., De Frenne, P., 2021. Microclimatic edge-to-interior gradients of European deciduous forests. Agric. Meteorol 311, 108699. https://doi.org/10.1016/J.AGRFORMET.2021.108699.
Meli, P., Ellison, D., Ferraz, S.F.d.B., Filoso, S., Brancalion, P.H.S., 2024. On the unique value of forests for water: hydrologic impacts of forest disturbances, conversion, and restoration. In: Global Change Biology, 30. John Wiley and Sons Inc. https://doi.org/10.1111/gcb.17162.
Menge, J.H., Magdon, P., Wöllauer, S., Ehbrecht, M., 2023. Impacts of forest management on stand and landscape-level microclimate heterogeneity of European beech forests. Landsc. Ecol 38 (4), 903–917. https://doi.org/10.1007/S10980-023-01596-Z/FIGURES/6.
Mildrexler, D.J., Zhao, M., Running, S.W., 2011. A global comparison between station air temperatures and MODIS land surface temperatures reveals the cooling role of forests. J. Geophys. Res 116 (G3), G03025. https://doi.org/10.1029/2010JG001486.
Mu, M., De Kauwe, M.G., Ukkola, A.M., Pitman, A.J., Guo, W., Hobeichi, S., Briggs, P.R., 2021. Exploring how groundwater buffers the influence of heatwaves on vegetation function during multi-year droughts. Earth. Syst. Dyn. 12 (3), 919–938. https://doi.org/10.5194/ESD-12-919-2021.
Mukul, S.A., Halim, M.A., & Herbohn, J. (2020). Forest Carbon Stock and Fluxes: Distribution, Biogeochemical Cycles, and Measurement Techniques (pp. 1–16). https://doi.org/10.1007/978-3-319-71065-5_23-1.
Nevins, L.M., Zambrano, J., 2024. Tree demographic and neighbourhood responses to regional environmental gradients of the northwestern United States. J. Ecol. 112 (1), 41–55. https://doi.org/10.1111/1365-2745.14217.
O'brien, R.M., 2007. A caution regarding rules of thumb for variance inflation factors. Qual. Quant 41 (5), 673–690. https://doi.org/10.1007/s11135-006-9018-6.
Palli, J., Mensing, S.A., Schoolman, E.M., Solano, F., Piovesan, G., 2023. Historical ecology identifies long-term rewilding strategy for conserving Mediterranean mountain forests in south Italy. Ecol. Appl. e2758. https://doi.org/10.1002/EAP.2758.
Palmer, W.C., 1965. Meteorological drought. Off. Climatol. Res,. Pap. (45).
Pavan, M., 1961. L'istituzione della Riserva naturale integrale di Poggio Tre Cancelli per la conservazione della «macchia mediterranea». Not. For. Mont. 6 (88), 2733–2734.
Peña-Claros, M., Nobre, C., 2023. A regional approach to save the Amazon. Science 381 (6664), 1261. https://doi.org/10.1126/SCIENCE.ADK8794.
Perino, A., Pereira, H.M., Navarro, L.M., Fernández, N., Bullock, J.M., Ceauşu, S., Cortés-Avizanda, A., Van Klink, R., Kuemmerle, T., Lomba, A., Pe'er, G., Plieninger, T., Benayas, J.M.R., Sandom, C.J., Svenning, J.C., Wheeler, H.C., 2019. Rewilding complex ecosystems. In: Science, 364. American Association for the Advancement of Science. https://doi.org/10.1126/science.aav5570.
Pesaresi, S., Biondi, E., Casavecchia, S., 2017. Bioclimates of Italy. J. Maps 13 (2), 955–960. https://doi.org/10.1080/17445647.2017.1413017.
Piovesan, G., Cannon, C.H., Liu, J., Munné-Bosch, S., 2022. Ancient trees: irreplaceable conservation resource for ecosystem restoration. Trends. Ecol. Evol. (Amst.) 37 (12), 1025–1028. https://doi.org/10.1016/J.TREE.2022.09.003.
QGIS Development Team, 2024. QGIS Geographic Information System. Open Source Geospatial Foundation Project. http://qgis.osgeo.org.
Ralhan, D., Keith, H., Pavlin, J., Stegehuis, A.I., Marchand, W., Fruleux, A., Poláček, M., Svitok, M., Nagel, T.A., Mikoláš, M., Kozák, D., Buechling, A., Dušátko, M., Janda, P., Chaskovsky, O., Roibu, C.C., Svoboda, M., 2023. Temperate primary forest biomass accumulates over centuries-long time frames. Ecosystems 1–18. https://doi.org/10.1007/S10021-023-00858-W/METRICS.
Sanczuk, P., Pauw, K.De, Lombaerde, E.De, Luoto, M., Meeussen, C., Govaert, S., Vanneste, T., Depauw, L., Brunet, J., Cousins, S.A.O., Gasperini, C., Hedwall, P.-O., Iacopetti, G., Lenoir, J., Plue, J., Selvi, F., Spicher, F., Uria-Diez, J., Verheyen, K., Frenne, De, P., 2023. Microclimate and forest density drive plant population dynamics under climate change. Nat. Clim. Chang 13 (8), 840–847. https://doi.org/10.1038/s41558-023-01744-y.
Santi, I., Carrari, E., De Frenne, P., Valerio, M., Gasperini, C., Cabrucci, M., Selvi, F., 2024. Impact of coppicing on microclimate and understorey vegetation diversity in an ancient Mediterranean oak forest. Sci. Total. Environ. 918, 170531. https://doi.org/10.1016/J.SCITOTENV.2024.170531.
Santos, E.G., Svátek, M., Nunes, M.H., Aalto, J., Senior, R.A., Matula, R., Plichta, R., Maeda, E.E., 2024. Structural changes caused by selective logging undermine the thermal buffering capacity of tropical forests. Agric. Meteorol 348, 109912. https://doi.org/10.1016/j.agrformet.2024.109912.
Senf, C., Seidl, R., 2021a. Mapping the forest disturbance regimes of Europe. Nat. Sustain. 4 (1), 63–70. https://doi.org/10.1038/S41893-020-00609-Y;SUBJMETA=158,2454,2808,631,706;KWRD=FOREST+ECOLOGY,GEOGRAPHY.
Senf, C., Seidl, R., 2021b. Persistent impacts of the 2018 drought on forest disturbance regimes in Europe. Biogeosciences 18 (18), 5223–5230. https://doi.org/10.5194/BG-18-5223-2021.
Sobrino, J.A., Jiménez-Muñoz, J.C., Paolini, L., 2004. Land surface temperature retrieval from LANDSAT TM 5. Remote. Sens. Env. 90 (4), 434–440. https://doi.org/10.1016/j.rse.2004.02.003.
Solano, F., Praticò, S., Piovesan, G., Chiarucci, A., Argentieri, A., Modica, G., 2021. Characterizing historical transformation trajectories of the forest landscape in Rome's metropolitan area (Italy) for effective planning of sustainability goals. Land. Degrad. Dev. 32 (16), 4708–4726. https://doi.org/10.1002/ldr.4072.
Suarez-Gutierrez, L., Müller, W.A., Marotzke, J., 2023. Extreme heat and drought typical of an end-of-century climate could occur over Europe soon and repeatedly. Commun. Earth. Environ. 4 (1), 415. https://doi.org/10.1038/s43247-023-01075-y.
Sungmin, O., Bastos, A., Reichstein, M., Li, W., Denissen, J., Graefen, H., Orth, R., 2022. The role of climate and vegetation in regulating drought–Heat extremes. J. Clim 35 (17), 5677–5685. https://doi.org/10.1175/JCLI-D-21-0675.1.
Sutherland, I.J., Bennett, E.M., Gergel, S.E., 2016. Recovery trends for multiple ecosystem services reveal non-linear responses and long-term tradeoffs from temperate forest harvesting. For,. Ecol,. Manage 374, 61–70. https://doi.org/10.1016/j.foreco.2016.04.037.
Tabacchi, G., Cosmo, L.Di, Gasparini, P., & Morelli, S. (2011). Stima Del Volume E Della Fitomassa Delle Principali Specie Forestali Italiene, Equazioni Di Previsione, Tavole Del Volume E Tavole Della Fitomassa Arborea Epigea.
Tarquini, S., Nannipieri, L., 2017. The 10 m-resolution TINITALY DEM as a trans-disciplinary basis for the analysis of the Italian territory: current trends and new perspectives. Geomorphology 281, 108–115. https://doi.org/10.1016/j.geomorph.2016.12.022.
Team, R. C., 2024. R: A language and Environment For Statisticalvcomputing. R Foundation for Statistical computing.
Thom, D., Sommerfeld, A., Sebald, J., Hagge, J., Müller, J., Seidl, R., 2020. Effects of disturbance patterns and deadwood on the microclimate in European beech forests. Agric. Meteorol 291, 108066. https://doi.org/10.1016/j.agrformet.2020.108066.
Urdiales-Flores, D., Zittis, G., Hadjinicolaou, P., Cherchi, A., Alessandri, A., Peleg, N., Lelieveld, J., 2024. A global analysis of historical and future changes in Mediterranean climate-type regions. Int. J. Climatol. 44 (15), 5607–5620. https://doi.org/10.1002/joc.8655.
Vacek, Z., Vacek, S., Cukor, J., 2023. European forests under global climate change: review of tree growth processes, crises and management strategies. J. Env.,. Manage 332, 117353. https://doi.org/10.1016/j.jenvman.2023.117353.
van der Schrier, G., Barichivich, J., Briffa, K.R., Jones, P.D., 2013. A scPDSI-based global data set of dry and wet spells for 1901–2009. J. Geophys. Res.:. Atmos. 118 (10), 4025–4048. https://doi.org/10.1002/jgrd.50355.
Vandewiele, M., Geres, L., Lotz, A., Mandl, L., Richter, T., Seibold, S., Seidl, R., Senf, C., 2023. Mapping spatial microclimate patterns in mountain forests from LiDAR. Agric. Meteorol 341. https://doi.org/10.1016/j.agrformet.2023.109662.
Wang, Z., Ginzler, C., Waser, L.T., 2020. Assessing structural changes at the forest edge using kernel density estimation. For,. Ecol,. Manage 456, 117639. https://doi.org/10.1016/j.foreco.2019.117639.
Weiss, A.D., 2001. Topographic position and landforms analysis. In: Poster presentation, ESRI User Conference.
Wells, N., Goddard, S., Hayes, M.J., 2004. A self-calibrating Palmer drought severity index. J. Clim 17 (12), 2335–2351. https://doi.org/10.1175/1520-0442(2004)017<2335:ASPDSI>2.0.CO;2.
Weng, Q., Gui, B., Peñuelas, J., Voogt, J., Bhardwaj, A., Sam, L., Yin, X., Shepherd, J., & Niyogi, D. (2025). Phenological Metrics in the Mitigation of Urban Heat: Timing and Thresholds. https://doi.org/10.21203/RS.3.RS-6948672/V1.
Williams, M.I., Dumroese, R.K., 2013. Preparing for climate change: forestry and assisted migration. J. For. 111 (4), 287–297. https://doi.org/10.5849/jof.13-016.
Wilson, M.F.J., O'Connell, B., Brown, C., Guinan, J.C., Grehan, A.J., 2007. Multiscale terrain analysis of multibeam bathymetry data for habitat mapping on the continental slope. Mar. Geod. 30 (1–2), 3–35. https://doi.org/10.1080/01490410701295962.
Wolf, C., Bell, D.M., Kim, H., Nelson, M.P., Schulze, M., Betts, M.G., 2021. Temporal consistency of undercanopy thermal refugia in old-growth forest. Agric. Meteorol 307, 108520. https://doi.org/10.1016/j.agrformet.2021.108520.
Wood, S.N., 2017. Generalized additive models: an introduction with R, second edition. Generalized Additive Models: An Introduction With R, 2nd Edition, pp. 1–476. https://doi.org/10.1201/9781315370279.
Wright, A.J., Francia, R.M., 2024. Plant traits, microclimate temperature and humidity: a research agenda for advancing nature-based solutions to a warming and drying

climate. Journal of Ecology. John Wiley and Sons Inc. https://doi.org/10.1111/1365-2745.14313.

Xu, X., Huang, A., Belle, E., Frenne, P.De, & Jia, G. (2022). Protected areas provide thermal buffer against climate change. https://www.science.org*Sci. Adv.* **8**, eabo0119. DOI:10.1126/sciadv.abo0119.

Yi, K., Smith, J.W., Jablonski, A.D., Tatham, E.A., Scanlon, T.M., Lerdau, M.T., Novick, K. A., Yang, X., 2020. High heterogeneity in canopy temperature among Co-occurring tree species in a temperate forest. J. Geophys. Res.:. Biogeosciences 125 (12). https://doi.org/10.1029/2020JG005892.

Zellweger, F., de Frenne, P., Lenoir, J., Vangansbeke, P., Verheyen, K., Bernhardt-Römermann, M., Baeten, L., Hédl, R., Berki, I., Brunet, J., van Calster, H., Chudomelová, M., Decocq, G., Dirnböck, T., Durak, T., Heinken, T., Jaroszewicz, B., Kopecký, M., Máliš, F., Coomes, D., 2020. Forest microclimate dynamics drive plant responses to warming. Science 368 (6492), 772–775. https://doi.org/10.1126/science.aba6880.

Zhang, Q., Barnes, M., Benson, M., Burakowski, E., Oishi, A.C., Ouimette, A., Sanders-DeMott, R., Stoy, P.C., Wenzel, M., Xiong, L., Yi, K., Novick, K.A., 2020. Reforestation and surface cooling in temperate zones: mechanisms and implications. Glob. Chang. Biol 26 (6), 3384–3401. https://doi.org/10.1111/gcb.15069.

Zhang, Z., Li, X., Liu, H., 2022. Biophysical feedback of forest canopy height on land surface temperature over contiguous United States. Environ. Res. Lett. 17 (3), 34002. https://doi.org/10.1088/1748-9326/ac4657.